makeTCR: A Modular Platform for Rapid, Scalable, Single-Step T Cell Receptor Synthesis

Authors

M. Hamberger*[1,2,3,4], M-T. Neuhoff*[1,2,3,5] C. Maldonado Torres[1,2,3], C. L. Tan[1,2,3,7], T. Boschert[1,2,3], A. Errerd[1,2,3,4], J. M. Lindner[8], M. Platten[1,2,3,4,6,7] , and E. W. Green[1,2,3]

1. German Cancer Research Center (DKFZ) Heidelberg, CCU Neuroimmunology and Brain Tumor Immunology, Germany.
2. German Cancer Consortium (DKTK), DKFZ, Core Center Heidelberg, Germany.
3. Department of Neurology, Medical Faculty Mannheim, MCTN, University of Heidelberg, Mannheim, Germany.
4. Faculty of Bioscience, University of Heidelberg, Heidelberg, Germany.
5. Faculty of Engineering Sciences, University of Heidelberg, Heidelberg, Germany.
6. Helmholtz Institute for Translational Oncology Mainz (HI-TRON Mainz), Mainz, Germany.
7. DKFZ-Hector Cancer Institute at the Medical Faculty Mannheim, University of Heidelberg, Germany.
8. BioMed X GmbH, Heidelberg, Germany

* Contributed equally, Correspondence e.green@dkfz-heidelberg.de

Author Contributions

- MH, TB and EWG developed the makeTCR system.
- MH, M-TN, CMT, CLT, TB, AE, JML and EWG performed experiments and designed figures.
- M-TN, EWG and CLT performed bioinformatic analyses.
- EWG conceived the work and wrote the manuscript with MH, M-TN and MP.

Competing interests

MP, CLT and EWG hold patents and PCT applications describing methods to identify tumor-reactive T cells, and are founders or employees of Tcelltech GmbH. JML is an employee of BioMed X GmbH.

Abstract

Personalised cell therapies utilising T cell receptors (TCRs) show tremendous clinical promise, though TCR synthesis and validation techniques lag far behind current TCR repertoire sequencing capacity. To address this gap we developed makeTCR: a modular TCR cloning system that enables rapid, single-step, 100% fidelity assembly of human or murine TCR sequences into diverse expression vectors. We provide pre-cloned modules for αβ and γδ TCRs, as well as many native and engineered constant regions. We show how implementing cell-free manufacturing both facilitates the propagation of precloned modules, and allows testable TCR material to be synthesised in 24 hours, enabling patient-derived TCRs to be prototyped prior to use in personalised cell therapies. makeTCR scales to making thousands of TCRs, at high fidelity and at substantially reduced cost. makeTCR is facilitated by a free, open-source, extensible, graphical platform to simplify, standardise, and accelerate TCR functionality testing for personalised medicine and beyond.

Introduction

Transgenic autologous T cell receptor (TCR) therapies are promising cancer immunotherapies in which a patient's T cells are genetically engineered to express a tumor-targeting TCR. First-generation transgenic TCR therapies utilise allogeneic TCRs to target recurrent epitopes, for example MAGE-A4 [1] in the case of the recently FDA approved afamitresgene autoleucel, or PRAME [2]. The clinical efficacy of these therapies demonstrates the potential of augmenting a patient's immune response. Identifying suitable TCRs has involved extensive screening campaigns to identify and characterise tumor-reactive TCRs, requiring single-cell sequencing to capture alpha and beta chain pairs [3,4]; the costs of this ensure that the majority of such off-the-shelf TCRs target epitopes are presented by the most common HLA-A*02:01 allele. For cancer patients with no recurrent target, or less frequent HLA allelotypes, it has been shown that patient-specific, tumor-reactive TCRs can be identified, in some cases resulting in remarkable remissions [3]. Such results raise the hope for autologous TCRs as broadly applicable therapies for patients; however, the median vein-to-vein time for developing such a therapy is over six months [4]. New low-cost, high-throughput paired TCR chain sequencing techniques [5], combined with statistical insights into T cell repertoire dynamics, are facilitating the identification of candidate TCRs based on TCR sequence alone [6], whilst we and others have shown that tumor-targeting TCRs can be rapidly identified from single cell sequencing data using gene expression signatures [7–11] or machine learning classifiers [12,13].

In addition to the need for rapid synthesis of therapeutic TCRs, there is increasing demand to generate and screen large TCR libraries to train machine learning models capable of predicting a TCR's cognate epitope [14,15], to identify the TCRs that sustain patient remission in TIL therapies [16], to identify the most effective therapeutic candidates among panels of TCRs targeting the same antigen [17], and to increase understanding the immune system dynamics. The generation of synthetic TCRs *de novo* from commercially sourced dsDNA fragments remains either expensive and low-throughput [18], or high-throughput but prone to generating pooled libraries with uneven clonotype distributions and high error rates, complicating screening campaigns [19]. TCR synthesis costs can be reduced by assembling pre-cloned libraries of germline V gene sequences with synthetic CDR3 and J gene sequences using either Golden Gate [20] or Gibson assembly [18,21]. Previous approaches were often multi-step, limited to αβ TCRs with no choice of delivery vector or TCR constant region, utilised cloning sites which have since been shown to result in low-fidelity assembly [22], and/or are not publicly available. Importantly, no existing solution provides software tools to automate the process of generating TCRs and quality control information from input TCR repertoire sequencing data. These factors limit the useability, cost, and ultimately throughput of TCR synthesis techniques.

Here, we present makeTCR, a modular, Golden Gate-based TCR cloning system utilising data-optimized assembly techniques [22] that enables single-step, 100% fidelity cloning of both αβ and γδ TCRs into an extensive collection of TCR expression vectors and (engineered) TCR constant domains. makeTCR is accompanied by a freely available, extensible, web-based

platform to automate the generation of TCRs from patient TCR repertoire sequencing results. We show how users can easily propagate hundreds of makeTCR modules using rolling circle amplification (RCA) in plate-based formats without deleterious effects on TCR assembly fidelity or error rate, that the makeTCR platform can generate novel TCRs in 24 hours for prototyping cell therapies, and that makeTCR scales to making thousands of TCRs at high fidelity for screening approaches at a fraction of current costs.

Results

High fidelity modular TCR assembly and broad vector support

We designed a series of mutually orthogonal Golden Gate overlaps to enable BsmBI mediated assembly of αβ and γδ TCRs as polycistronic transcripts by combining pre-cloned modules encoding germline TR*V and TR*C sequences with *de novo* synthesised CDR3-TR*J fragments (Fig. 1a). By utilising data-optimized assembly techniques [22] and silent codon mutagenesis we created a set of overlaps predicted to result in 100% assembly fidelity for both αβ and γδ TCRs (Fig. 1b, c). We also generated 100% fidelity solutions for TR*V genes whose amino acid sequences precluded the use of the standard overlaps (Extended Data Fig. 1a). We experimentally validated assembly fidelity by partitioning a bacterial construct expressing the blue chromoprotein amilCP [23] into six modules matching the cohesive ends used for alpha/beta TCR assembly; blue/white screening of the resultant transformant *E. coli* confirmed 99.9% assembly fidelity (Extended Data Fig. 2a). We further utilised our modular amilCP test system to rapidly benchmark modified Golden Gate thermocycling protocols, creating a protocol that doubled assembly yield compared to the manufacturer's recommendations (Extended Data Fig. 2b).

Having established the fidelity of our design, we generated plasmids encoding domesticated forms of human and murine TRAV, TRBV, TRGV, and TRDV germline genes flanked by appropriate BsmBI recognition sites (see Methods and full sequences in Supplementary Data Tab. 1). We also created plasmids encoding a range of commonly used human and murine TCR constant genes, including engineered forms that limit cross-pairing with endogenously expressed TCRs by incorporating disulfide mutations [24] or switched transmembrane domains [25], as well as variants modules including selection markers mStaygold2 or puromycin N-acetyltransferase to facilitate enrichment or selection of TCR transgenic cells. Finally, we generated a module co-expressing human TR*C and CD3z, which has been shown to increase the amount of surface-expressed TCR, allowing for more sensitive screening for antigen-specific T cell function [26].

In order to support the broadest range of use cases, we adapted a series of commonly used TCR expression vectors to the makeTCR system for Golden Gate cloning, allowing single-step cloning of TCRs into expression plasmids supporting TCR expression utilising lentivirus, adeno-associated virus (AAV), sleeping beauty transposon, and homology directed repair (HDR) plasmids targeting the human TRAC and the AAVS1 safe harbour loci (Fig. 1a, Extended Data

119 Fig. 3). We also accommodated existing TCR expression systems by providing a vector
120 containing flanking attL sites to allow shuttling of makeTCR assembled sequences into
121 Gateway™ vectors using Invitrogen's LR Clonase II system. Lastly to facilitate subcloning TCRs
122 generated using the makeTCR system we used silent mutagenesis to remove occurrences of
123 the IIs enzymes PaqCI (human modules) or BsaI (murine modules) to make these available for
124 downstream cloning. To maximize TCR assembly fidelity, we incorporated a unique SwaI
125 restriction enzyme site in all vectors: in the backbone of TR*V and TR*C modules and in the
126 filler region of TCR expression vectors, allowing unassembled input material to be linearised
127 following TCR assembly reactions, thereby preventing undesired input carryover. Taken
128 together, these design features confer high cloning fidelity, flexibility, and reusability.

129 **Simple software platform to facilitate TCR manufacture**

130 To facilitate the use of makeTCR we designed a free, open-source graphical software interface
131 to streamline the process of generating the *de novo* synthesized CDR3-TR*J DNA sequences
132 required for modular TCR assembly (Fig. 2a). We support repertoire files from the commonly
133 used 10X Genomics' Single Cell Immune Profiling solution, as well as the emerging AIRR-C
134 standard utilised by other single cell profiling platforms through MiXCR [27]. All software options
135 are extensively documented with modal help documentation to assist users in selecting
136 between the various engineered TCR constant regions and vectors available (Fig. 2b, c).

137 The makeTCR software selects TCRs to be cloned from the repertoire file based on either an
138 uploaded list of target CDR3 sequences, the frequency of TCR clonotypes, or a desired
139 quantity of randomly selected TCRs. Users then select the desired TR*C domains and TCR
140 expression vector from drop-down lists; new modules can be easily integrated into makeTCR
141 software in a code-free manner by uploading a fasta formatted sequence using a defined
142 naming schema. The makeTCR software then generates the synthetic CDR3-TR*J DNA
143 sequences that must be generated for each TCR, as well as TCR cloning instructions based on
144 the 96 well plate assignments of the appropriate TR*V, TR*C and vector modules in both
145 human readable and automation compatible formats (Supplementary Data Tab. 1). makeTCR
146 outputs the CDR3-TR*J DNA sequences in multiple formats allowing users to choose a
147 synthesis technique best suited to their target application and the DNA synthesis services
148 locally available. Since a fraction of TCRs natively contain long homopolymer runs in the CDR3-
149 TR*J regions (Fig. 2d), makeTCR offers to remove these by silent mutagenesis to facilitate
150 downstream TCR screening assays based on sequencing; makeTCR also generates TCR vector
151 maps to facilitate cloning quality control and provide reference information for sequencing-
152 based screens.

153 **Rolling circle amplification simplifies propagation of makeTCR modules**

154 The modular makeTCR collection requires the preparation of >100 plasmids from bacterial
155 cultures; a labour- and space-intensive process that is challenging to automate. In contrast
156 randomly primed, Phi29 mediated RCA is a simple, inexpensive, high-fidelity method to

157 propagate plasmid DNA at concentrations similar to a bacterial midiprep [28]. RCA reactions are
158 isothermal, compatible with plate-based automation, and facilitate the preparation of
159 equimolar products as the extreme processivity of engineered Phi29 tends to generate similar
160 yields. We tested whether the distribution and maintenance of makeTCR modules could be
161 simplified by RCA mediated DNA propagation without affecting TCR assembly fidelity or TCR
162 sequence error rate using our modular amilCP system (Fig. 3a). We found that amilCP
163 assemblies showed a similar error rate (number of white colonies) when assembling plasmid-
164 encoded or RCA-amplified templates (P=0.391, Fig. 3b). We also observed similar yields (total
165 number of colonies, P=0.087, Fig. 3c), with a slight trend towards fewer colonies when using
166 RCA amplified input, likely due to randomly primed RCA amplification resulting in a fraction
167 of amplicons containing only a single BsmBI site precluding full assembly.

168 To determine whether RCA templates were prone to particular types of error we sequenced
169 a number of white colonies from each assembly. We found errors indicating non-synonymous
170 SNPs in amilCP, amilCP truncations as a result of bacterial recombination, and amilCP mis-
171 assemblies when using both RCA or plasmid encoded templates (Extended Data Fig. 4). As
172 several of the SNPs were shared between the RCA and plasmid assemblies, and the error rate
173 was higher than previously observed, we reasoned that these SNPs must have been present
174 in the source plasmid at levels undetectable by commercial Sanger and Nanopore plasmid QC
175 sequencing. By examining Nanopore plasmid sequencing reads we could confirm that the
176 most common SNP in both assemblies was indeed a rare variant already present in the input
177 plasmid material (Fig. 3d), and not the result of RCA. As our functional assay for assembly
178 fidelity utilising amilCP might over-estimate errors due to the selective advantage conferred
179 on *E. coli* not expressing amilCP (Fig. 3f), we also performed Nanopore-based amplicon
180 sequencing on completed amilCP assemblies. This showed a small increase in SNPs when
181 using RCA amplified templates (99.18% perfectly aligning reads vs 99.97% using plasmid
182 encoded templates, Fig. 3e), confirming previous observations [29]. Given this low error rate,
183 we performed all TCR assembly experiments using RCA amplified TR*V and TR*C modules.

184 **makeTCR enables rapid, cell-free TCR prototyping in 24 hours**

185 We previously created a machine learning classifier, predicTCR [12], to identify tumor-reactive
186 TCRs from single-cell sequenced tumor infiltrating lymphocytes (TILs) in an antigen-agnostic
187 fashion in minutes, rather than through extensive TCR screening campaigns [4]. We set out to
188 similarly accelerate the prototyping of such patient-derived TCRs prior to *in vivo* use to further
189 reduce autologous T cell therapy manufacturing time. As proof of concept we used TIL data
190 from the previously described 'BT21' brain metastasis of a melanoma patient [12]. We used an
191 enzymatic DNA synthesizer to generate complementary oligonucleotides encoding the CDR3-
192 TR*J domains for seven CD8+ TCR clonotypes which predicTCR classified as being tumor-
193 reactive and which had not previously been tested. We also generated two TCRs previously
194 shown to be dominantly (ct9) or weakly (ct8) localised in the membrane of T cells when
195 expressed as human/mouse chimeric TCRs (positive and negative controls respectively) [12].

196 Synthesized oligonucleotides were annealed and assembled with appropriate makeTCR
197 modules, allowing us to complete cell-free (and therefore endotoxin-free) manufacture of
198 mRNA encoding candidate tumor-reactive TCRs within 24 hours (Fig. 4a); by comparison,
199 previously reported approaches would take over a week to generate a synthetic TCR
200 (Supplementary Data Table 2).

201 We validated the accuracy of the rapid makeTCR process by Nanopore sequencing the Golden
202 Gate assembled IVT template, finding over 90% reads to be free of sequence errors (Fig. 4b).
203 Upon electroporation into healthy donor T cells, we found two of the seven newly cloned
204 TCRs dominantly occupied the T cell membrane (% mTCRb+ expression, Fig. 4c) and conferred
205 reactivity against the BT21 tumor cell line even in presence of the endogenous TCR (Fig. 4d).
206 The responsiveness of TCR ct9 was consistent with its reactivity when expressed as a fully
207 human TCR (commercially synthesised as a sequence-verified plasmid with a 3-week
208 turnaround) in a functional reporter assay using the T-FINDER system [30] (Extended Data Fig.
209 5), underscoring the variety of applications makeTCR can accelerate and enhance.

210 **makeTCR mediated manufacture of large synthetic TCR libraries**

211 Given the increasing demand for large numbers of synthetic TCRs for both basic and
212 translational research, we developed a variant of makeTCR to support high-throughput, low-
213 cost TCR synthesis (Fig. 5a). We encoded the CDR3-TRAJ and CDR3-TRBJ sequences as linked,
214 BsmBI flanked sequences bracketed by a unique pair of mutually orthogonal primer
215 sequences [31] as a 250-base oligonucleotide (Fig. 5b, Extended Data Fig. 6a,b). This allowed
216 unique TCR regions to be synthesised using inexpensive pooled oligonucleotide synthesis
217 technology, before recovery from the pool by PCR. Utilising 96 primers (to simplify integration
218 with liquid handling systems utilising plates) allows for 4,560 unique primer pairs; at this scale
219 each oligonucleotide can be synthesised for less than €1 (Fig. 5c). By assembling the CDR3-
220 TR*J encoding oligos with makeTCR modules the overall TCR manufacturing cost is less than
221 €3.50 (Extended Data Fig. 6c) – well below the cost of conventional TCR cloning (€80-200).
222 We adapted the demultiplexing protocol published by Subramanian et al. for use with the
223 high-yield, low-GC bias KAPA HiFi polymerase to minimize primer off-target annealing and
224 ensure selective, high-yield amplification (Extended Data Fig. 7a). We found that cooled PCR
225 setup was essential to minimize the activity of the polymerase's 3'-5' exonuclease activity
226 truncating primers, and utilised a high primer annealing temperature to promote specific
227 amplification of target oligos.

228 As proof of concept, we used the makeTCR platform to clone two libraries of patient derived
229 αβ TCRs (n=1761 and n=380 respectively) using the high-throughput approach. TCRs were
230 cloned into a third-generation lentiviral transfer vector, pooled, transformed into
231 electrocompetent *E. coli*, and prepared as a TCR library. Nanopore long read sequencing of
232 the TCR libraries revealed a median of 83.2% and 80.0% of reads mapping to a correctly
233 assembled TCR (Fig. 5d), with errors representing both dropouts (missing TCRs) and
234 incorrectly paired CDR3 regions. We found that this occurred as a result of off-target primer

235 binding amplifying multiple oligonucleotides during the demultiplexing step (Extended Data
236 Fig. 7b-e), and that the placement of length-normalising filler DNA sequence within the
237 oligonucleotide sequence ensured that misassemblies more frequently contained an
238 incorrect CDR3a-TRAJ than CDR3b-TRBJ (Extended Data Fig. 6, Extended Data Fig. 8). Overall
239 we found that high-throughput arrayed assembly of TCRs using makeTCR resulted in a tight
240 distribution of TCR frequencies suitable for downstream functional screening (Fig. 5e,f).

241 Discussion

242 The diversity of transgenic TCR therapies in development is rapidly increasing, in part due to
243 the much broader range of targets available to TCRs relative to chimeric antigen receptors
244 (CARs), but also due to the decreasing costs of transgenic cell manufacture [32]. However, the
245 TCR field has not yet coalesced around a rapid, high-fidelity synthesis solution that enables
246 simple, low-cost, scalable yet flexible manufacture of TCRs. We addressed these limitations
247 with the makeTCR platform, which we built to meet the needs of researchers working across
248 different model systems and therapeutic contexts, enabling consistent and reliable TCR
249 assembly of both αβ and γδ TCRs, for both human and murine sequences. By utilising data-
250 optimized Golden Gate assembly design techniques [22], makeTCR allows for versatile
251 assemblies of VDJ regions grafted onto a TCR constant region of choice without compromising
252 assembly fidelity. Furthermore, makeTCR enables standardized TCR generation regardless of
253 downstream application by providing compatible vectors for all commonly used TCR
254 expression systems. We demonstrate the utility of using Phi29-mediated RCA to substitute
255 for traditional bacterial culture in propagating makeTCR modules, representing a practical
256 advance that reduces the labour and resources required to maintain a modular plasmid
257 collection while retaining TCR assembly fidelity.

258 A key limitation of previous TCR synthesis techniques was the lack of a software platform to
259 automate the process of generating TCRs from information contained in TCR repertoire
260 datafiles. We developed a free, extensible, open-source graphical platform that allows
261 researchers to upload repertoire sequencing data, select which TCRs they wish to clone, and
262 receive all required DNA sequences, cloning instructions, and vector maps for performing
263 quality control sequencing. The platform supports both the rapid and high-throughput
264 makeTCR variants reported here, but can also be used to generate full V(D)J sequences to
265 facilitate TCR cloning without utilising makeTCR's precloned V gene modules. The software
266 platform is available at https://makeTCR.com, can be run locally (in case of data privacy
267 issues), and can easily be expanded in a code-free manner by users who wish to use novel
268 modules – for example TR*C domains linked to suicide switches enabling the targeted
269 depletion of TCR transgenic cells [33].

270 We have demonstrated that makeTCR enables rapid prototyping of TCRs: novel, patient-
271 derived, tumor-reactive TCRs could be identified, manufactured and functionally validated
272 within 48 hours – a process that previously took multiple weeks [34]. This illustrates the
273 potential of this approach for prioritising patient-derived TCRs with optimal properties such

274 as dominant membrane expression for personalised clinical applications. Our results are
275 particularly timely given the recent FDA 'Fast Track' designation for mRNA encoded TCRs as a
276 monotherapy for HBV-related hepatocellular carcinoma (NCT05195294). This suggests that
277 pipelines combining makeTCR's rapid TCR assembly with cell-free, GMP grade, endotoxin-free
278 manufacture of mRNA or DNA doggybones [35] could further accelerate - and thereby reduce
279 the cost of - personalised TCR therapies.

280 We show that makeTCR scales to manufacturing libraries of 1000s of TCRs with fidelity at or
281 greater than previously reported approaches [19], but with lower TCR distribution bias and less
282 codon optimisation. makeTCR thereby provides a cost effective TCR manufacturing platform
283 to enable the large-scale functional screening of TCRs that will be required to leverage
284 machine learning techniques to the problems of identifying and designing TCRs with desired
285 antigen specificity, affinity, and signalling properties. Overall, we found that 77.7% of TCRs in
286 Library 1 and 71.1% in Library 2 were assembled with at least 70% fidelity. Given that TCR
287 misassemblies are primarily the result of imperfect demultiplexing of the oligonucleotide pool
288 this suggests that fidelity improvements could be made by switching polymerase, using open-
289 source PCR buffers that do not contain reagents to stabilise primer annealing, and utilising
290 primers containing 3' phosphorothioate bonds to prevent primer trimming. As long read
291 sequencing resolves both CDR3 domains of manufactured TCRs, deliberately mixing oligos to
292 shuffle the CDR3 domains prior to screening is a strategy to generate data exploring the
293 respective importance of each CDR3 domain to epitope binding. Supporting this, a recent
294 analysis [36] of TCR-epitope prediction tools showed that while in most cases tools performed
295 better when using both CDR3a and CDR3b sequences, for some epitopes one chain almost
296 entirely defined epitope binding. This suggests that further high-throughput experimentation
297 enabled by makeTCR will generate data to elucidate such structure-function relationships and
298 train future epitope prediction models.

299 To facilitate such studies, and the use of makeTCR by the broader TCR research community,
300 all TR*V and TR*C gene modules and makeTCR compatible vectors are available from both
301 Addgene and the European Plasmid Repository.

302 # Figures

303 **Figure 1: modular, high fidelity Golden Gate TCR assembly system using makeTCR**

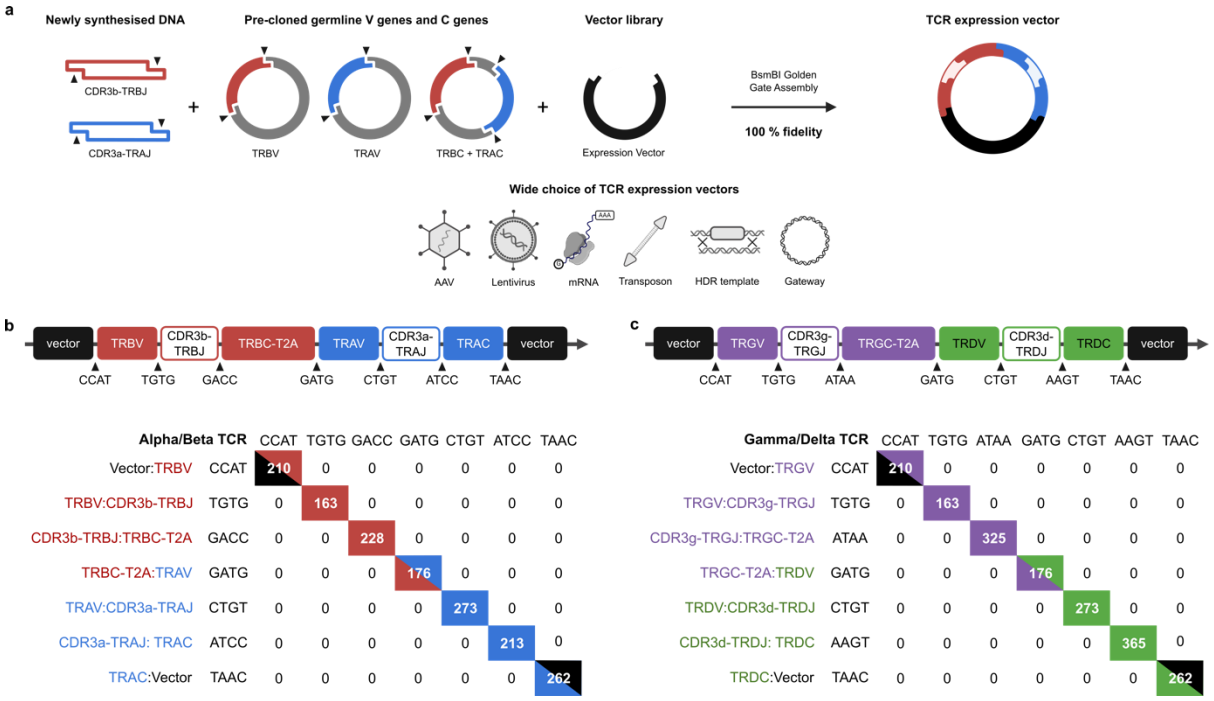

Alpha/Beta TCR	CCAT	TGTG	GACC	GATG	CTGT	ATCC	TAAC
Vector:TRBV	CCAT	210	0	0	0	0	0	0
TRBV:CDR3b-TRBJ	TGTG	0	163	0	0	0	0	0
CDR3b-TRBJ:TRBC-T2A	GACC	0	0	228	0	0	0	0
TRBC-T2A:TRAV	GATG	0	0	0	176	0	0	0
TRAV:CDR3a-TRAJ	CTGT	0	0	0	0	273	0	0
CDR3a-TRAJ: TRAC	ATCC	0	0	0	0	0	213	0
TRAC:Vector	TAAC	0	0	0	0	0	0	262

Gamma/Delta TCR	CCAT	TGTG	ATAA	GATG	CTGT	AAGT	TAAC
Vector:TRGV	CCAT	210	0	0	0	0	0	0
TRGV:CDR3g-TRGJ	TGTG	0	163	0	0	0	0	0
CDR3g-TRGJ:TRGC-T2A	ATAA	0	0	325	0	0	0	0
TRGC-T2A:TRDV	GATG	0	0	0	176	0	0	0
TRDV:CDR3d-TRDJ	CTGT	0	0	0	0	273	0	0
CDR3d-TRDJ: TRDC	AAGT	0	0	0	0	0	365	0
TRDC:Vector	TAAC	0	0	0	0	0	0	262

304

305 **a**, Schematic for the makeTCR system of BsmBI mediated modular Golden Gate assembly of
306 TCRs using pre-cloned germline TR*V and TR*C genes, a panel of compatible TCR expression
307 vectors, and newly synthesised DNA oligonucleotides encoding the CDR3-TR*J regions. **b**,
308 schematic of an assembled polycistronic alpha/beta TCR expression construct and table
309 showing the expected 100% fidelity ligation results (adapted from NEB's Ligase Fidelity
310 Viewer® [22]). **c**, expected ligation results as in b but showing an assembled gamma/delta TCR.
311 **a**, Created using BioRender.com.

312

313 **Figure 2: makeTCR software interface**

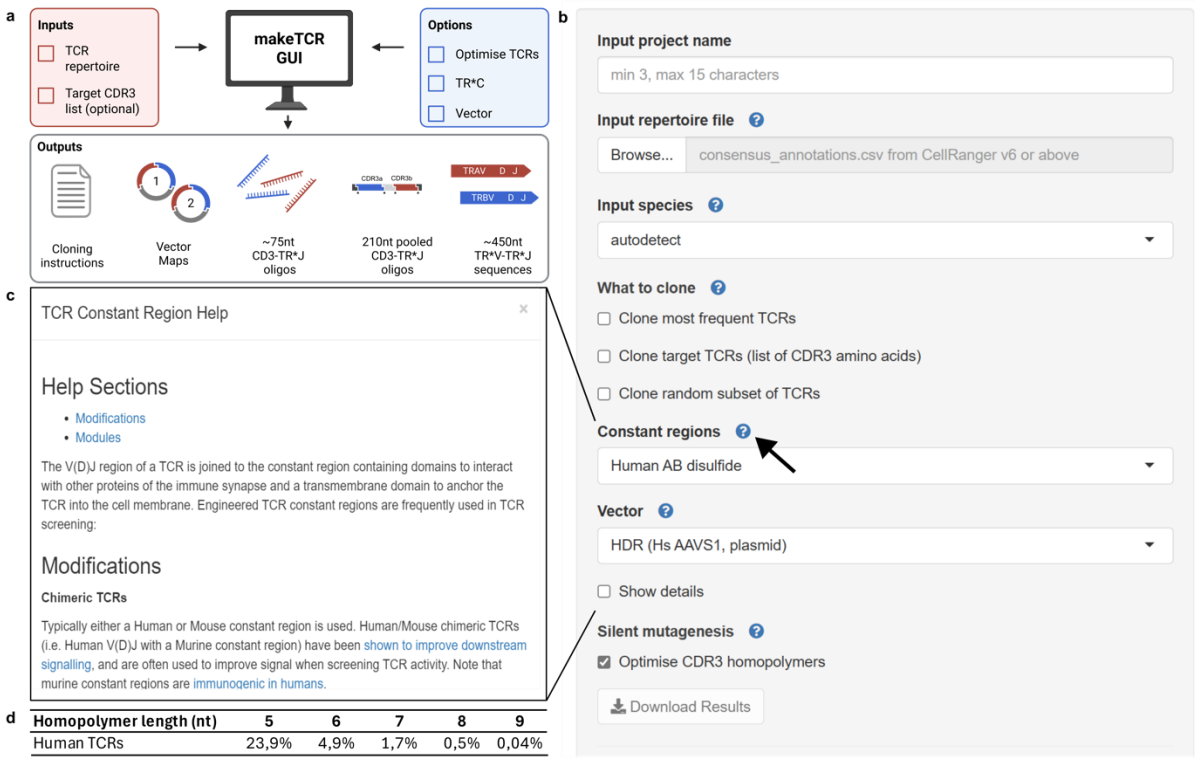

Homopolymer length (nt)	5	6	7	8	9
Human TCRs	23,9%	4,9%	1,7%	0,5%	0,04%

314

315 **a**, Schematic of the makeTCR software platform: users upload TCR repertoire files and
316 optionally a list of target CDR3 sequences, set the desired TR*C domains and expression
317 vector, and choose whether to codon optimise TCR nucleotide homopolymer sequences. The
318 makeTCR platform generates cloning instructions, vector maps, and files detailing the CDR3-
319 TR*J nucleotide sequences to be synthesised. makeTCR outputs instructions for cloning using
320 short oligos, pooled oligos, and fully synthetic VDJ domains (see Fig. 4 and 5). **b**, the makeTCR
321 graphical interface utilises simple UI elements to guide users, with each option accompanied
322 by a detailed help section (arrow). **c**, example help popup to guide TCR constant domain
323 selection (including links to the scientific source literature). **d**, CDR3-TR*J regions from TCRs
324 derived from a human TIL repertoire natively contain nucleotide homopolymer runs which
325 can be difficult to sequence; makeTCR can deplete such homopolymers by silent mutagenesis.
326 **a**, Created using BioRender.com.

Figure 3: RCA amplification of input modules does not affect TCR cloning fidelity.

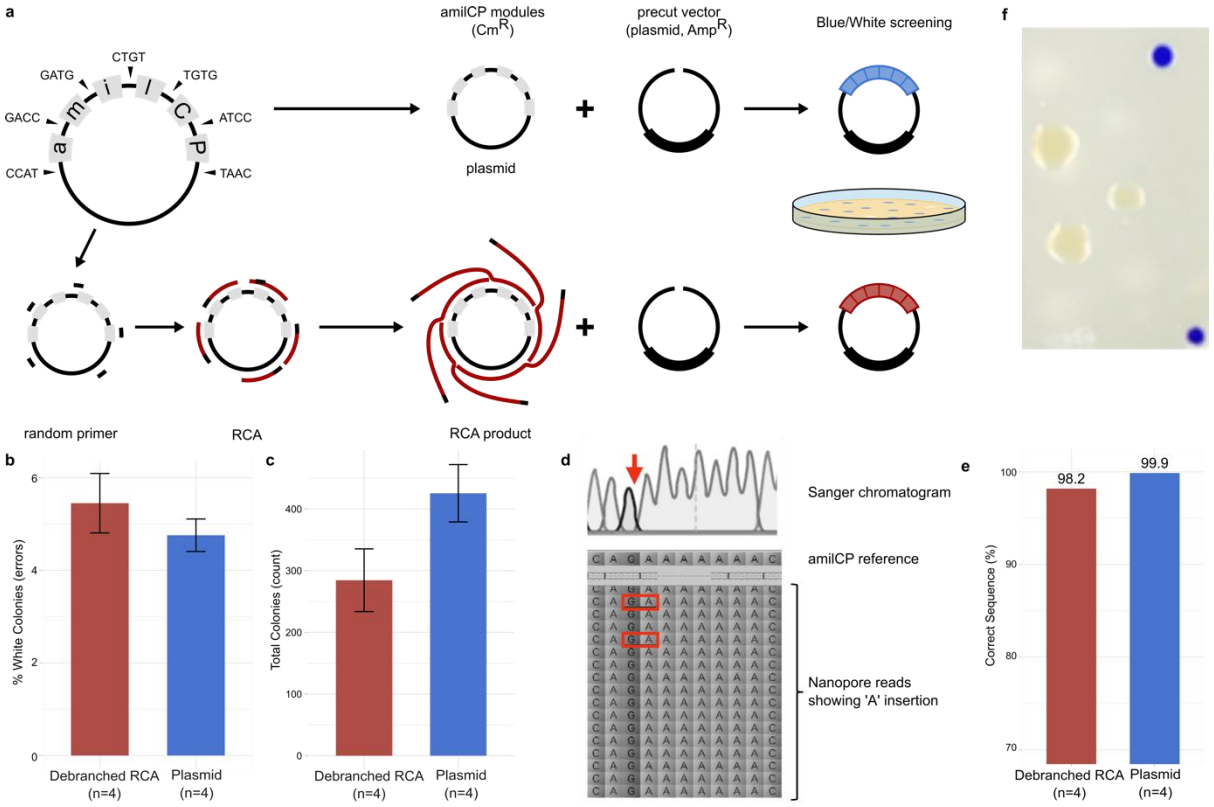

a, A plasmid pre of a bacterial amilCP expression cassette split into six BsmBI flanked modules was further amplified by RCA and debranched. Both RCA and plasmid templates were then assembled into a destination vector using BsmBI mediated Golden Gate assembly, transformed into *E. coli* and the blue/white ratio of resulting colonies counted. **b**, no significant difference in the overall fidelity (number of blue vs white colonies) was found when using plasmid or RCA amplified input (P=0.391, Welch Two Sample t-test, n=4 replicates per template type). **c**, Golden Gate assembly using RCA encoded modules trended toward a lower yield than using plasmid encoded modules (P=0.087, Welch Two Sample t-test, n=4 replicates per condition. **d**, NGS was used to confirm that the most common SNP (a frameshifting addition of an A base, red boxes) was present in the source plasmid miniprep DNA at a level below that detectable by either Sanger sequencing (red arrow) or the whole plasmid nanopore sequencing consensus, but could be found in individual reads. **f**, we confirmed previous reports that expression of amilCP from high-copy plasmids imposes at least a 25 % fitness cost on *E. coli* hosts (small blue colonies vs large white colonies)[23], exerting a selective pressure to limit amilCP expression and translation. **e**, Nanopore sequencing of completed Golden Gate assembly reaction product shows that RCA amplified plasmids exhibit a minor increase in number of SNPs (99.97% perfect reads vs 98.18% respectively).

Figure 4: Rapid makeTCR mediated TCR Assembly and TCR Prototyping

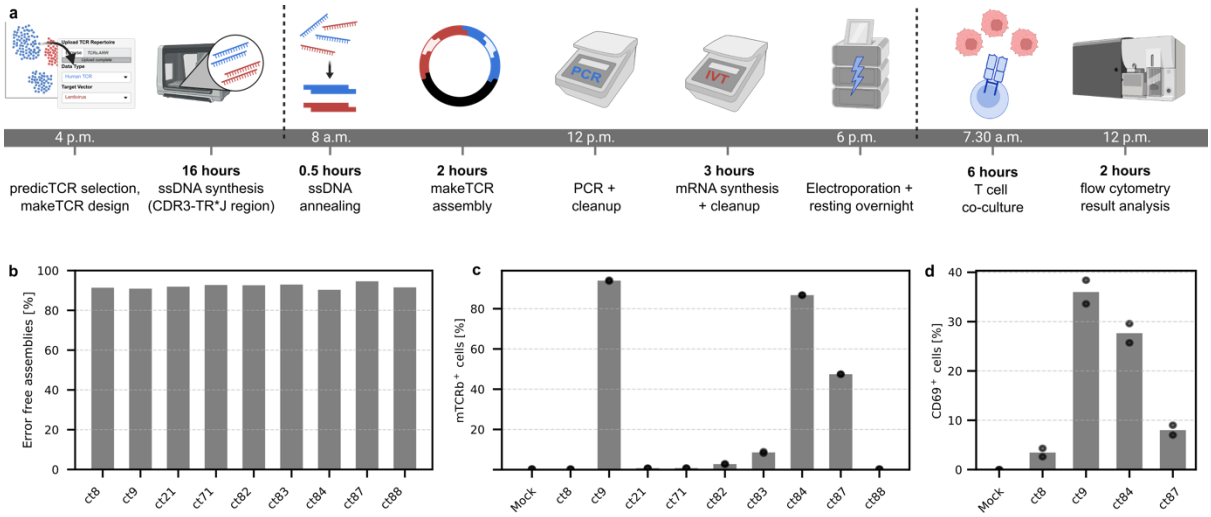

a, Schematic diagram of rapid TCR manufacture and testing using an on-site enzymatic oligonucleotide synthesizer and makeTCR modules. The makeTCR software platform generates oligo sequences for TCRs (such as those identified using predicTCR) which are synthesised overnight. Oligos are pooled, annealed and assembled with appropriate TR*V, TR*C and vector modules. The assembled polycistronic TCR is PCR amplified to yield a template for IVT, generating mRNA for electroporation into T cells in an entirely cell-free process. TCR testing – for example by co-culture with a target cell line - can commence the next day. **b**, Nanopore sequencing of nine TCRs (ct8-ct88) generated using the rapid makeTCR protocol found >90% of reads were error-free. **c**, expression of nine $CD8^+$ TCRs derived from the BT21 TIL population as polycistronic human/mouse chimeric TCRs in healthy donor REP T cells revealed that test TCR clonotypes ct84 and ct87 show dominant membrane localisation (determined by the murine $mTCRb^+$) even in the presence of endogenous TCR chains with human constant regions. Previously characterised 'dominant' (ct9) and 'weakly' presented TCRs (ct8) included as positive and negative controls respectively. **d**, Co-culture of transgenic REP T cells with the BT21 tumor cell line confirmed the predicted anti-tumor reactivity of ct84 and ct87, as well as the ct9 positive control, as assessed by expression of the early activation marker CD69. **a**, Created using BioRender.com.

Figure 5: High-Throughput, Oligo-pool mediated makeTCR Assembly

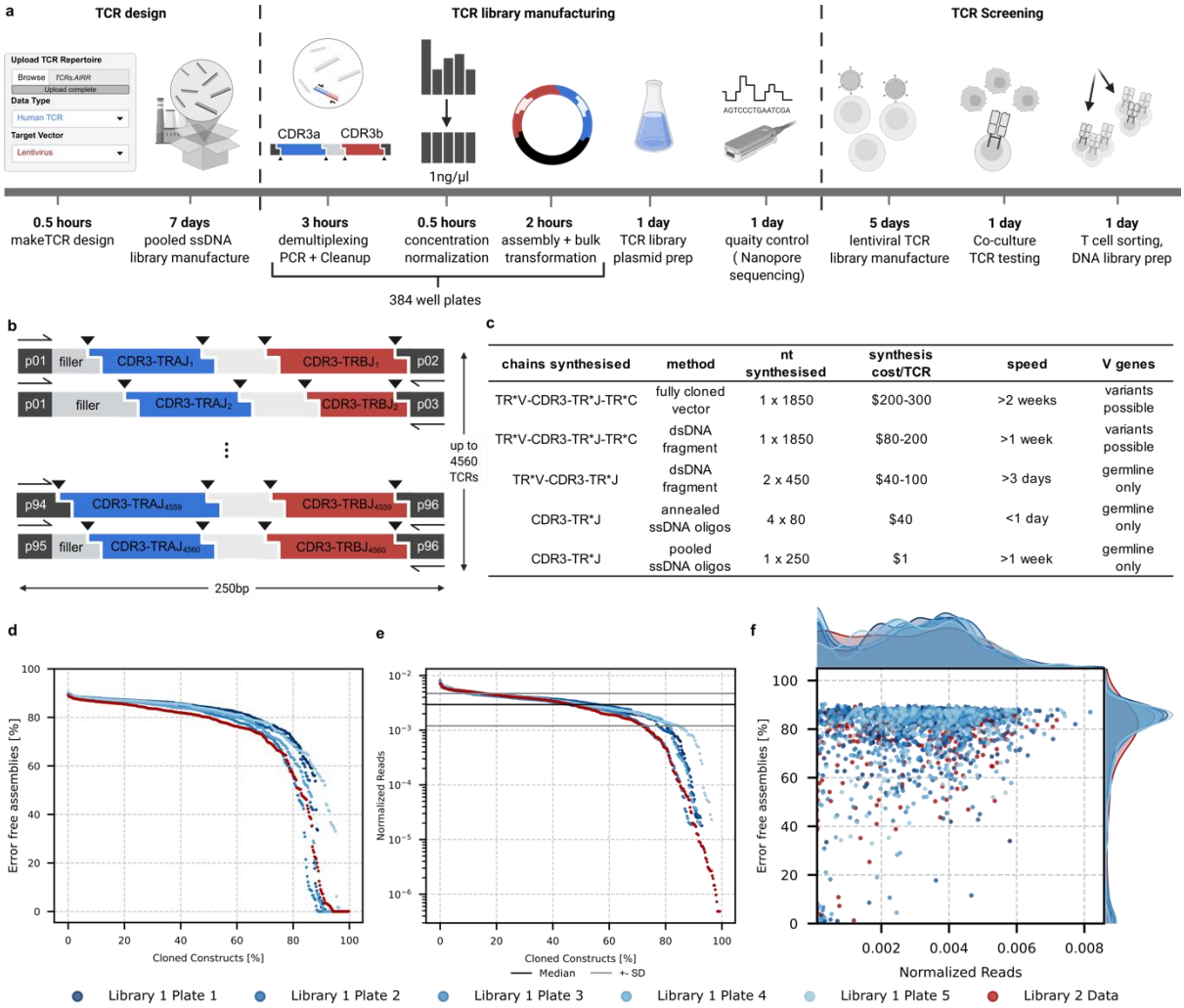

chains synthesised	method	nt synthesised	synthesis cost/TCR	speed	V genes
TR*V-CDR3-TR*J-TR*C	fully cloned vector	1 x 1850	$200-300	>2 weeks	variants possible
TR*V-CDR3-TR*J-TR*C	dsDNA fragment	1 x 1850	$80-200	>1 week	variants possible
TR*V-CDR3-TR*J	dsDNA fragment	2 x 450	$40-100	>3 days	germline only
CDR3-TR*J	annealed ssDNA oligos	4 x 80	$40	<1 day	germline only
CDR3-TR*J	pooled ssDNA oligos	1 x 250	$1	>1 week	germline only

a, Schematic illustrating the use of makeTCR to manufacture 1000s of TCRs by demultiplexing pooled ssDNA oligonucleotides. The makeTCR software platform encodes CDR3a-TRAJ and CDR3b-TRBJ pairs as a 250 nt oligonucleotide flanked by a unique pair of mutually orthogonal primer binding sites. Individual oligos are demultiplexed, cleaned and normalised in 384 well plates, before being assembled in miniaturised Golden Gate reactions with appropriate TR*V, TR*C and vector backbone modules. Assembled TCRs are pooled and transformed into *E. coli* to amplify the final TCR library. Nanopore sequencing mediated quality control is performed before the library can be used for TCR screening as previously described [19]. **b**, schematic of pooled oligos showing the use of filler sequences to normalise oligo length to 250 nt; 96 unique primers enable up to 4,560 CDR3-TR*J encoding oligos to be specifically amplified from the pool. **c**, comparative costs of different methods of synthesising TCRs, ranging from commercial synthesis of the full ~1,850 nt polycistronic TCR transcript to utilising pools of 250 nt CDR3-TR*J encoding oligos. Additional cloning costs for synthesised TCRs are <€3/TCR (Extended Data Fig. 6c). **d**, for each TCR the percentage of aligned Nanopore reads representing a correctly assembled TCR are plotted; TCRs are coloured according to the 384 well plate used for their assembly. **e**. Distribution of reads aligning to TCRs within each library, coloured by source plate. Reads were normalized to the total read count per library, showing

384 a tight distribution of TCRs with some dropouts. **f**, dot plot and density plots combining **d** and
385 **e**. **a**, **b**, Created using BioRender.com.

Extended Data

Extended Data Fig. 1: makeTCR Golden Gate Assembly Fidelities

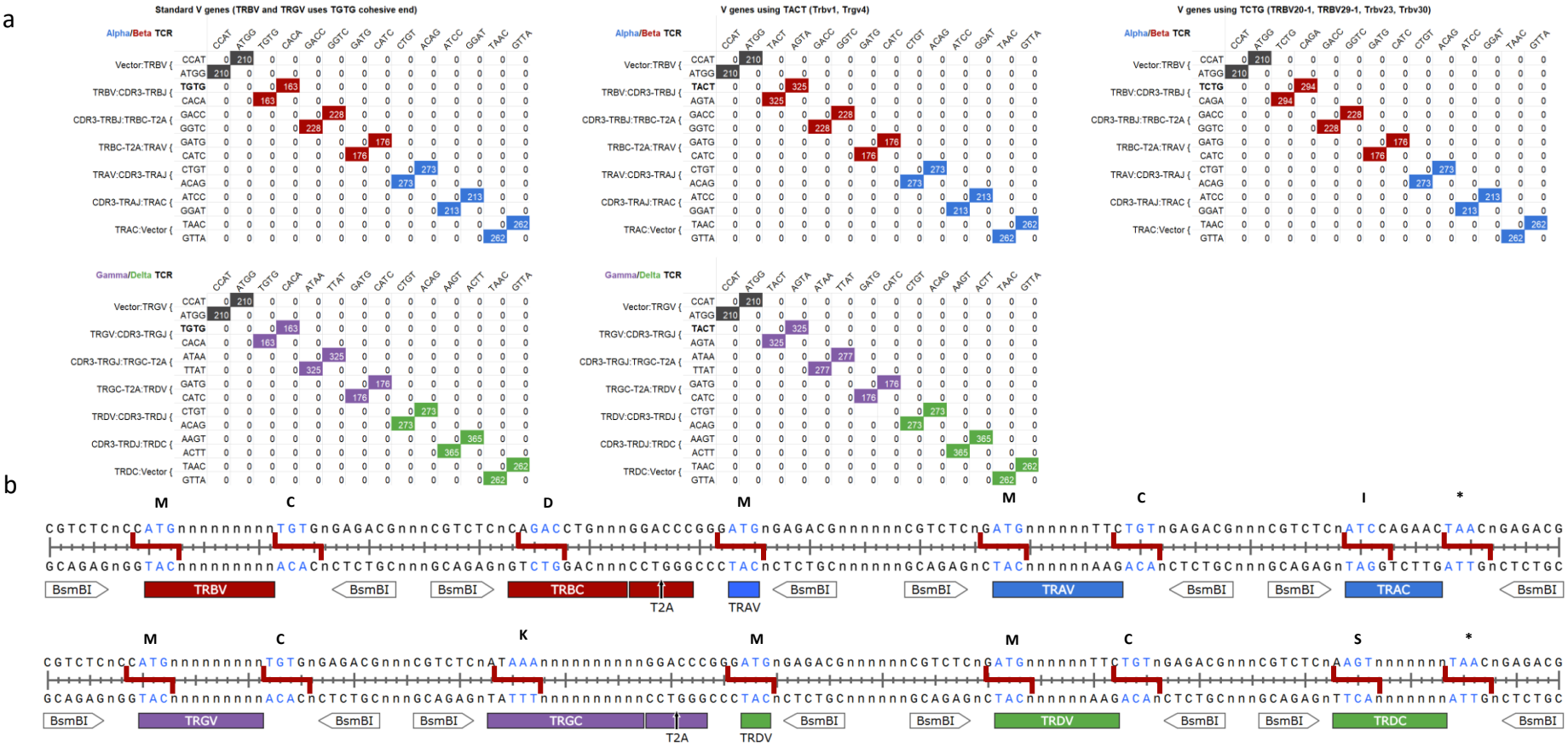

a, Golden Gate fidelity matrices for all makeTCR assemblies; note exceptions where the V gene amino acid sequence does not allow for the use of the TGTG cohesive end to join TRBV or TRGV to its CDR3 region. Genes coloured as in Fig. 1a. **b,** position of cohesive ends relative to gene sequence: blue DNA bases denote the nucleotides encoding the methionine and cysteine that define the ends of each V gene, as well as the first and last complete codon of each constant gene module. Red lines show cohesive ends generated by the IIs enzyme BsmBI (sites in white).

393 **Extended Data Fig. 2: Validating assembly fidelity**

394

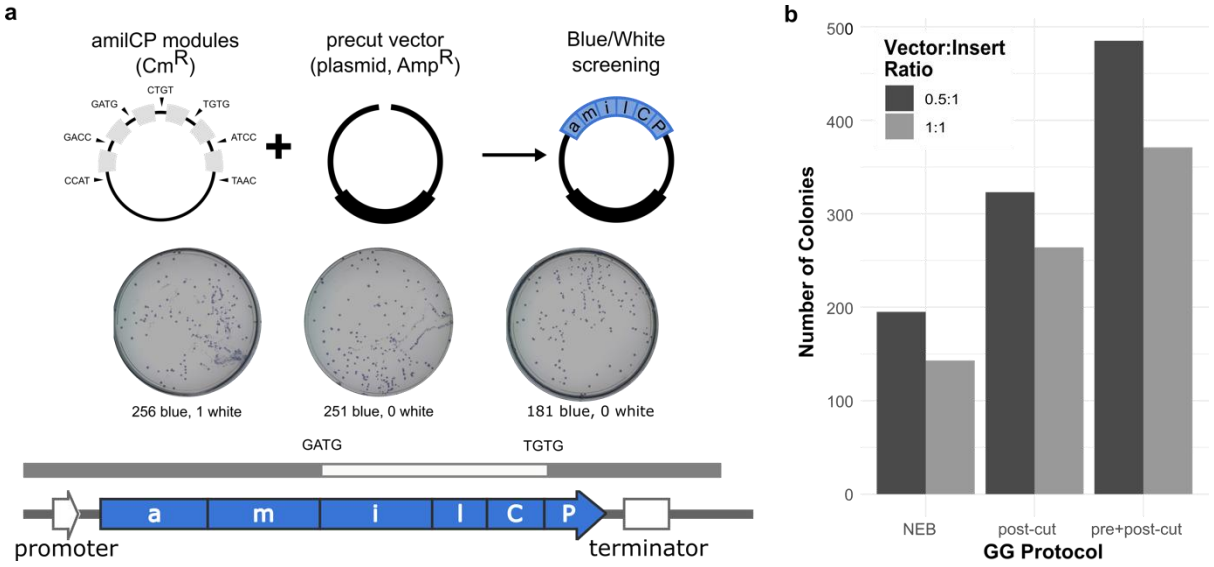

395

396 **a**: the predicted 100% Golden Gate assembly fidelity of the cohesive ends selected to
397 assemble an alpha/beta TCR from modules was experimentally verified by splitting a bacterial
398 amilCP expression cassette into BsmBI flanked modules linked by the same 4 nt cohesive ends.
399 The assembled product was transformed into *E. coli*, resulting in 688 blue colonies (i.e. amilCP
400 expressing) and 1 white colony – an assembly fidelity of 99.9%. The single white colony was
401 sequenced to show a mis-assembly linking the cohesive ends GATG and TGTG. **b**, modular
402 assembly of the amilCP expression cassettes was used to test variant BsmBI mediated Golden
403 Gate assembly thermocycling protocols; a variant protocol with pre- and post-assembly
404 thermal soak steps resulted in a twofold increase in yield (number of blue colonies).

405 **Extended Data Fig. 3: makeTCR TCR expression vectors**

406

407 **a,** Lentiviral transfer vector; TCR expression driven by long EF1a promoter, truncated LTRs are
408 used to satisfy higher biosafety requirements. **b,** AAV vector; TCR expression driven by CMV
409 promoter. **c,** Gateway^{TM} pENTR compatible vector. **d,** Sleeping Beauty transposon vector; TCR
410 expression driven by EF1a promoter. **e,** Vector for HDR mediated integration into the Human
411 genome at the TRAC locus; TCR driven by endogenous promoter and product cleaved using
412 E2A sequence. **f,** Vector for HDR mediated integration into the Human genome at the AAVS1;
413 TCR driven by endogenous promoter and product cleaved using E2A sequence. **g**: AAV
414 packaging compatible variant of **e**. **h**: guide for generating custom TCR expression vectors
415 compatible with makeTCR cloning.

416

Extended Data Fig. 4: RCA and plasmid miniprep templates result in similar error profiles in Golden Gate assemblies

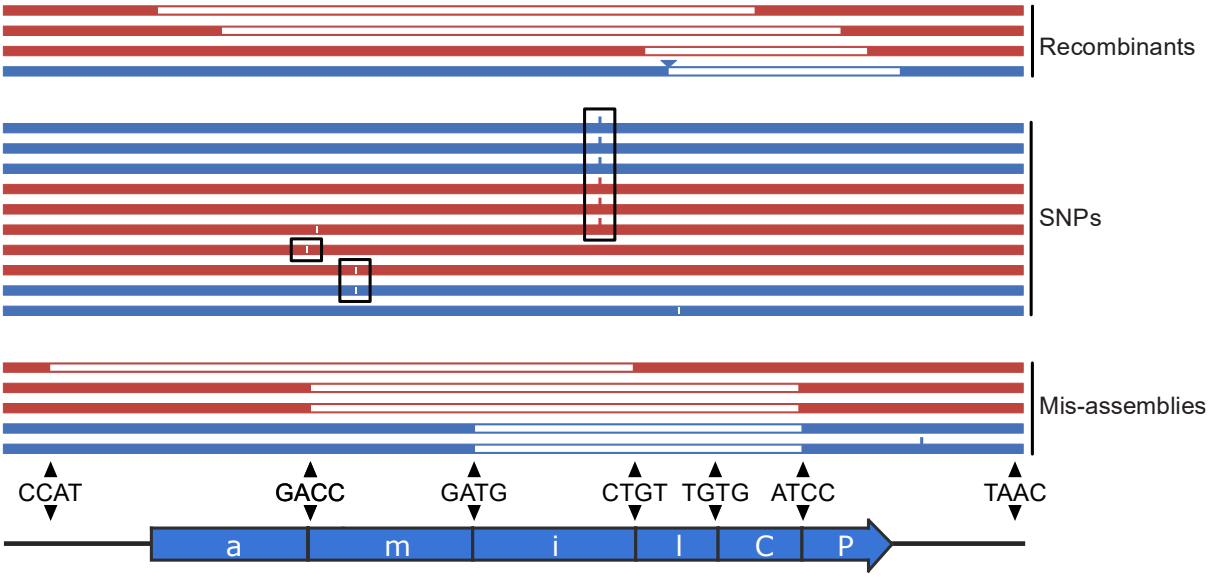

White colonies from Golden Gate mediated amilCP assembly using RCA encoded (red) or plasmid encoded (blue) modules (Fig. 3) were Sanger sequenced. For both template types we found colonies representing amilCP truncated by bacterial recombination (partial modules missing), single nucleotide polymorphisms (SNPs, raised lines representing nucleotide insertions, gaps representing missing nucleotide) and Golden Gate mis-assemblies (complete modules missing). SNPs that resulted in premature stop codons indicated by black boxes. SNPs shared between plasmid and RCA plasmid assemblies were found to be present in the plasmid prior to Phi29 mediated amplification (see Fig. 3 for details).

428 **Extended Data Fig. 5: Reactivity of commercially cloned TCR ct9 against BT21**

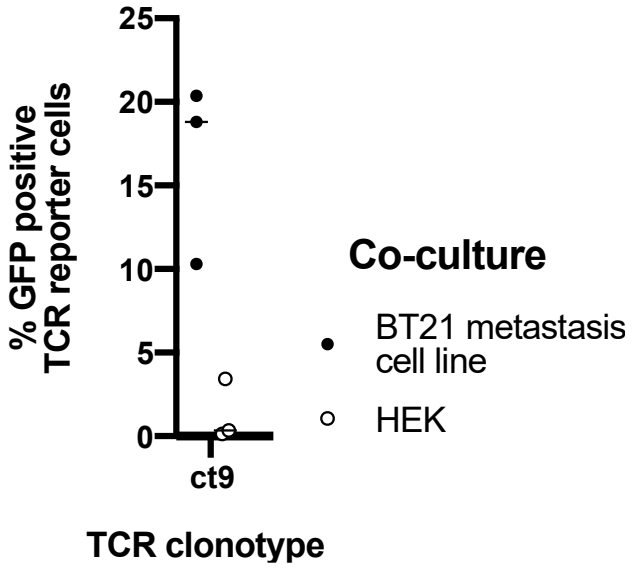

429

430 The coding sequence of BT21 TCR clonotype ct9 was commercially manufactured as a
431 polycistronic TCR (~1.8kb) in a lentiviral expression vector, packaged to generate functional
432 lentiviral particles and transduced into Jurkat cells containing the T-FINDER fluorescent
433 reporter of T cell activation [30] and a cassette expressing the human co-receptor CD8.
434 Transgenic T cells were activated upon co-cultivation with the BT21 metastasis cell line but
435 not HEK cells, confirming BT21 reactivity of this TCR clonotype.

436 **Extended Data Fig. 6: Example of a high-throughput makeTCR oligonucleotide and pricing breakdown**

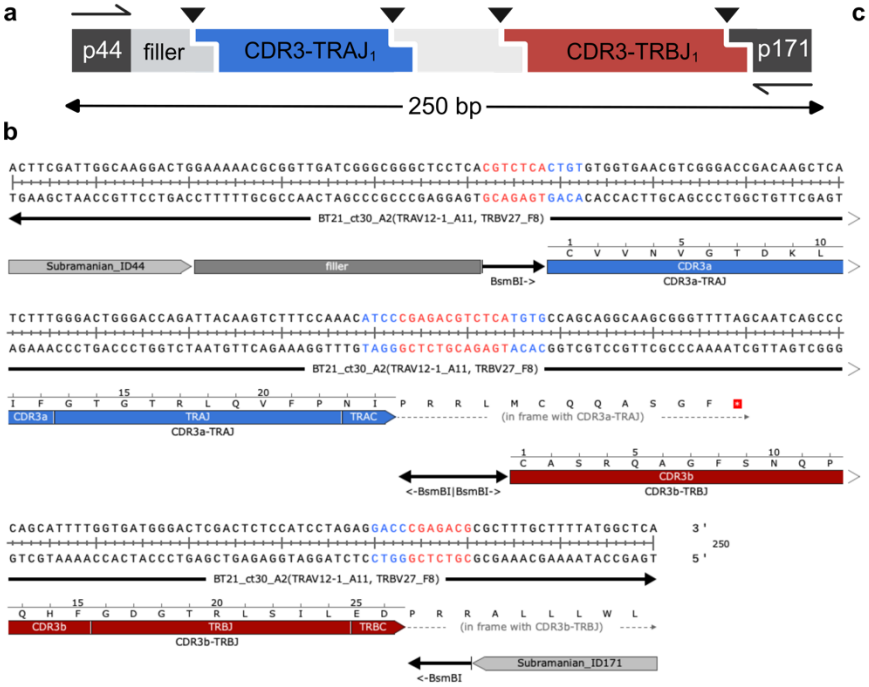

c

Process	Category	Item	2 µl reaction	384 plate
Template	Oligos	250nt ssDNA oligonucleotide	€ 1.00	€ 384.00
PCR	Oligos	Demultiplexing oligos	€ 0.10	€ 38.40
PCR	Plastics	Dispendix S100 primer plates	€ 0.09	€ 35.00
PCR	Enzymes	Kapa Hifi 15µl	€ 0.39	€ 151.20
PCR	Plastics	Twin.tec 384 PCR (0030128532)	€ 0.02	€ 6.80
PCR	Plastics	PCR seal (0030127781) (2x)	€ 0.00	€ 1.36
PCR	Plastics	Integra tips (primer transfer)	€ 0.04	€ 13.80
Cleanup	Beads	Ampure beads	€ 0.12	€ 47.58
Cleanup	Plastics	Agilent Reservoir	€ 0.01	€ 2.40
Cleanup	Plastics	UV Star plate (Greiner 781801)	€ 0.04	€ 15.63
Cleanup	Plastics	Fluotics 70µl filter tips, 6 per well	€ 0.57	€ 219.60
Cleanup	Plastics	PCR seal (0030127781) (1x)	€ 0.00	€ 1.36
Assembly	Plastics	Fluotics 30µl tips	€ 0.08	€ 29.87
Assembly	Plastics	PCR seal (0030127781) (3x)	€ 0.01	€ 4.08
Assembly	Enzymes	BsmBI v2 HF (E1602L)	€ 0.71	€ 270.95
Assembly	Plastics	Twin.tec 384 PCR plate (0030128532)	€ 0.02	€ 6.80
			€ 3.20	**€ 1,228.82**

437

438 **a,** schematic of a 250nt oligo encoding makeTCR compatible CDR3-TRAJ and CDR3-TRBJ regions. **b,** nucleotide sequence of an example oligo
439 sequence (shown as a dsDNA post PCR amplification product, BsmBI sites highlighted in red, cohesive ends in blue). **c**, costs of high-throughput
440 makeTCR assemblies when generating 2000 TCRs per manufacturing run. **a**, Created using BioRender.com.

Extended Data Fig. 7: Oligonucleotide demultiplexing optimisation and QC

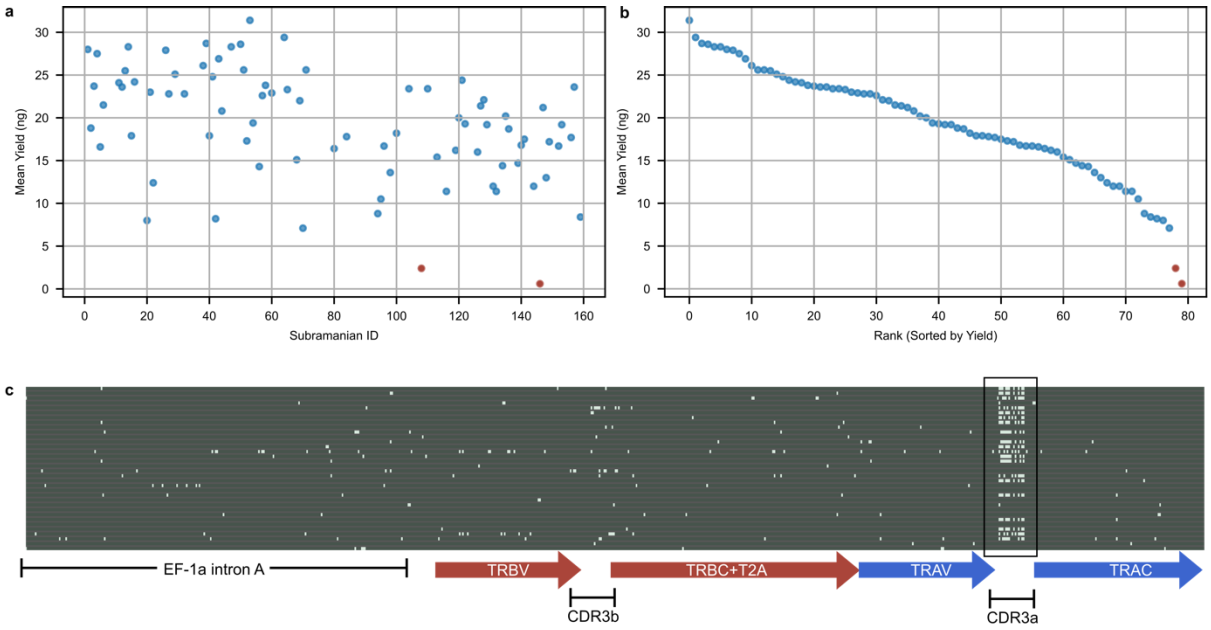

d

Reference	CDR3a	CDR3b	Reads	P1 ID	P2 ID
Lib 2 H08	**CAVSKGSSNTGKLIF**	**CSARYQGPAPYQETQYF**	**32,317**	**39**	**184**
Lib 2 B16	CAVYNQGGKLIF	CASSAVGQGILGAFF	6,775	**39**	183
Lib 2 F06	CAGYSGGGADGLTF	CASSLGLYNEQFF	2,142	**39**	160
Lib 2 M24	CAMREFQGAQKLVF	CASSLQDLNTEAFF	1,551	41	116
Lib 2 H01	CAVRDDKIIF	CASSLSKGQKAFF	1,551	113	**184**

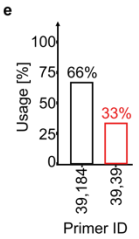

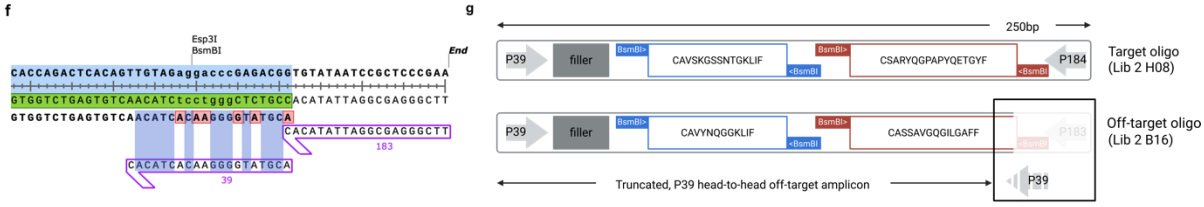

a, **b,** the orthogonal demultiplexing primers reported by Subramanian et al. were benchmarked across 1000s of PCR reactions demultiplexing TCRs from different pooled oligonucleotide libraries to determine the mean performance of each primer. Primers that performed poorly in our high Tm demultiplexing PCR (e.g. primer IDs 108 and 146, red dots) were excluded from further use. **c.** Example alignments of Nanopore sequencing reads to a low quality assembled TCR (Lib 2 H08); alignments show that the assembled TCR contains correctly dispensed vector, TRBV, TRBC, TRAV and TRAC modules, but a proportion of incorrect oligo-encoded CDR3a sequences (white regions – see black box). **d.** Nanopore sequencing of the demultiplexing PCR product revealed four off-target amplicons, 3 of which shared designed binding sites for primer 39. **e.** Flexiplex analysis of amplicons identified 66 % of reads contained the on-target primer sequences (39,184), whilst 33 % of reads contained head-to-head orientated instances of primer 39 (39,39) closely resembling the alignment result in d. **f,** detailed view of off-target amplicon Lib 2 B16 designed to be amplified by primers 39 and 183. Despite only matching 13 / 20 nucleotides primer 39 was able to bind the

457 oligonucleotide in an off-target location, resulting in amplification mediated solely by primer
458 39 (with the mismatched terminal 'C' nucleotide likely being removed by KAPA HiFi's 3'-5'
459 proofreading activity). This off-target binding destroyed the BsmBI site required to generate
460 the GACC cohesive end required to assemble the Lib 2 B16 CDR3b sequence, thus TCR
461 assemblies contain the correct CDR3b but incorrect CDR3a. **g.** schematic of d, black box
462 indicates region shown in panel f. **g**, Created using BioRender.com.

463 **Extended Data Fig. 8: High-throughput makeTCR library assembly QC results**

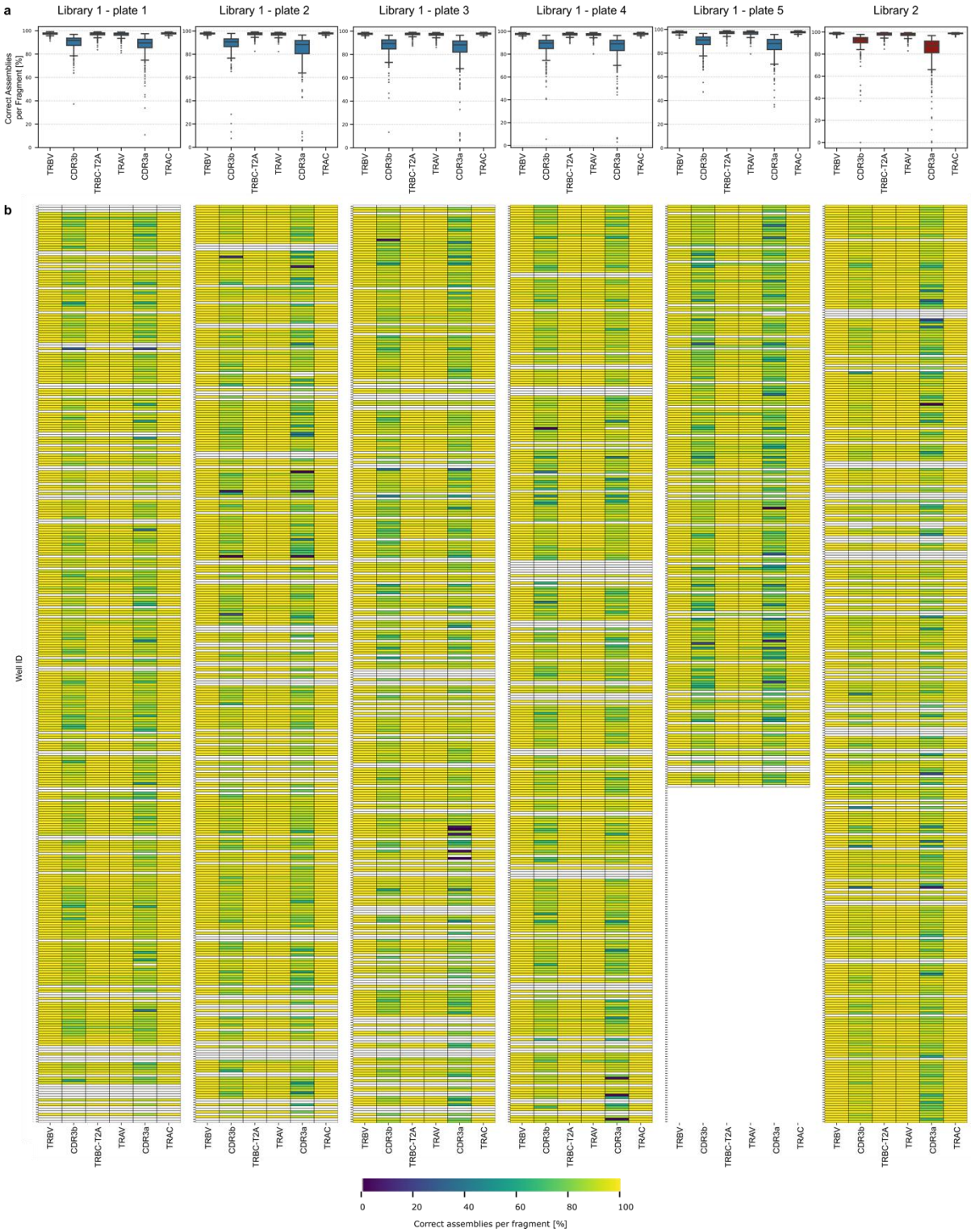

464

465 **a**. Percent reads per reference that align to the correct segment (TRBV, CDR3b, TRBC+T2A,
466 TRAV, CDR3a, TRAC) subdivided by 384 well plate on which they were cloned. The lowest 20
467 % quantile by reads was filtered to remove cloned TCRs with insufficient reads for accurate
468 assessment. Note lower fidelity of CDR3a assembly, as described in Extended Data Fig. 8. **b**.
469 Heatmap of each reference per plate and the corresponding percentage of reads per
470 reference that map to the right segment (TRBV, CDR3b, TRBC+T2A, TRAV, CDR3a, TRAC). The

471 lowest 20 % quantile by reads was filtered to remove cloned TCRs with insufficient reads for
472 accurate assessment.

473 ## Supplementary Data

474 **Supplementary Data Tab. 1: makeTCR Germline V Module Sequences**

475 makeTCR modules are distributed on three 96 well plates: 'p2_Hs_V' containing the Human TRAV and TRBV germline modules, 'p 3_Mm_V'
476 containing the Trav and Trbv modules for cloning Murine TCRs, and 'p 4_GD_misc' containing the modules for Human and Mouse gamma/delta
477 TCRs, as well as additional TR*C modules, vectors and uncommonly used Murine germline Trav modules. Addgene_id = Addgene plasmid
478 number, EPR_id = European Plasmid Repository plasmid number.

479 *(included as separate file due to table size)*

Supplementary Data Tab. 2: Comparison of TCR synthesis and cloning methods

Addgene (https://www.addgene.org/), EPR = European Plasmid Repository (https://www.plasmids.eu). HT = high-throughput.

	Time	Cost	Throughput	Software	Addgene	EPR	Fidelity	TCRs	Species	TR*Cs	Vectors
Hu et al 2018 [20]	7 days	$$$$	<100	No	Yes	No	+	AB	Human	Hs.TR*C	Lentivirus
Xia et al 2022 [37]	14 days	$$$$	<100	No	No	No	-/+	AB	Human	Hs.TR*C	Lentivirus
Afeyan et al 2024 [34]	14 days	$$$$	<100	No	Yes	No	++(+)	AB	Human	Mm.TR*C	Lentivirus
Moravec et al 2024 [19]	14 days	$	1000	No	No	No	++	AB	Human, (Mouse)	Mm.TR*C	Lentivirus, Retrovirus
makeTCR	1 day (fast), 16 days (HT)	$$	1-2000	Yes	Yes	Yes	+++	AB, GD	Human, Mouse	Diverse, expandable	Lentivirus, AAV, HDR, Gateway, Transposon, + others

483 **Supplementary Data Tab. 3 Subramanian primers mean yield**

484 Scaled mean PCR yield per Subramanian primer when demultiplexing individual
485 oligonucleotides from pooled oligonucleotide libraries.

primer_id	scaled_mean_yield	uses	primer_id	scaled_mean_yield	uses
1	21.4	36	104	17.7	45
2	19.8	36	110	20.9	44
3	20.1	38	113	14.0	47
4	21.3	38	116	15.8	44
5	15.4	39	119	15.8	47
6	19.0	37	120	19.6	46
11	19.1	34	121	21.3	46
12	17.7	35	122	18.1	50
13	19.2	34	126	17.1	48
14	22.4	34	127	19.1	47
15	17.9	36	128	20.3	46
16	19.8	37	129	16.5	25
21	19.8	42	131	13.1	45
26	19.9	44	134	16.0	44
27	16.2	46	135	18.9	45
29	20.4	46	136	17.0	45
32	19.4	47	139	20.2	50
38	19.1	44	140	17.6	47
39	20.9	45	141	16.7	47
40	17.1	46	144	12.8	47
41	19.0	49	147	19.5	45
43	19.7	47	148	15.2	46
47	19.5	44	149	17.5	41
50	19.9	43	152	15.6	41
51	17.4	43	153	17.5	37
52	16.0	41	156	18.7	39
53	22.1	42	157	22.3	37
54	15.6	42	22	11.8	17
56	16.5	42	44	17.2	17
57	20.0	43	160	16.1	15
58	18.8	41	163	16.9	14
60	20.1	45	164	18.0	14
64	22.9	44	167	14.7	12
65	21.2	46	170	16.1	13
68	12.9	44	171	20.0	12
69	19.1	46	172	19.0	12
71	22.0	47	174	16.6	12
80	15.6	46	175	15.5	13
84	17.7	45	177	17.6	13
94	11.7	47	180	20.1	12
95	14.0	47	181	17.8	10

98	13.3	45	183	20.8	15
100	17.5	47	184	15.9	13

Material availability

Human germline TRAV and TRBV plasmids, as well as a selection of TR*C plasmids and makeTCR compatible vectors, have been submitted as 96 well plate plasmid collection to Addgene (www.addgene.org) – see Supplementary Data Table 1, plate '2_Hs_V'.

Murine germline TRAV, TRBV, TRGV and TRDV plasmids, Human TRGV and TRDV, and an extensive collection of TR*C modules and expression vectors are available from the European Plasmid Repository (www.plasmids.eu) – see Supplementary Data Table 1, plates '3_Mm_V' and '4_GD_Misc'.

Code availability

The makeTCR service is available at https://makeTCR.com, and on publication the source code will be made freely available at https://gitlab.com/EdGreen21/makeTCR.

Acknowledgements

- We gratefully acknowledge the data storage service SDS@hd supported by the Ministry of Science, Research and the Arts Baden-Württemberg (MWK) and the German Research Foundation (DFG) through grant INST 35/1503-1 FUGG and INST 35/1503-1 FUGG as well as the German Cancer Research Center Next Generation Sequencing and Flow Cytometry Core Facilities.
- The German Ministry of Education and Science (National Center for Tumor Diseases Heidelberg NCT 3.0 program 'Precision immunotherapy of brain tumors' and the DKTK program) to MP (DKTK equipment grant).
- Federal Ministry of Education and Research (BMBF) and the Ministry of Science Baden-Württemberg, Excellence Strategy of the Federal and State Governments of Germany EMS, flagship 'Engineering Molecular Systems' spotlight proposal 'Synthetic Immunology' and 'Sequencing Oligo Libraries' (ExU 6.1.9).
- Hector Cancer Institute Seed Funding Program to MP, project 445549683,
- M-TN is supported by the Vector Stiftung (P2024-0750).
- CLT is supported by a DKFZ Hector Seed Funding Kick-start EarlyCareer fellowship (C-3PO).
- TB is supported by the Helmholtz-Institute for Translational Oncology Mainz (HI-TRON Mainz) as by a German Cancer Consortium DKTK, DKFZ Joint Funding project award (TRUST) to MP.
- MP received funding from the European Research Council (ERC) under the European Union's Horizon Europe project 101141901.
- We gratefully acknowledge Dr Kim Boonekamp for help preparing figures.

521 ## Online Methods

522 **Design and testing of optimal Golden Gate overlaps for TCR assembly**

523 Mutually orthogonal Golden Gate overlaps for assembling TCRs as polycistronic transcripts
524 were iteratively designed to bracket the methionine at the start of TR*V genes, the Cysteine
525 residue defining the CDR3 region, the first complete amino acid of TR*C, and either the end
526 of a T2A linker (for TRBC-T2A and TRGC-T2A) or a TAA encoded stop codon (for TRAC and
527 TRDC) with help of NEB's web tools [22] and targeted silent mutagenesis. The final overlaps are
528 shown in Extended Data Fig. 1.

529 **Golden Gate assembly fidelity assays using amilCP**

530 We codon optimised the coral *Acropora millepora* chromoprotein amilCP for expression in
531 *E.coli*, splitting the coding sequence into six modules linked by the same Golden Gate overlaps
532 and flanked by BsmBI recognition sites as used to make an αβ TCR (CCAT, TGTG, GACC, GATG,
533 CTGT, ATCC, TAAC). amilCP expression was driven by the constitutive bacterial promoter
534 BBa_J23110 and terminated by the *E. coli* histidine operon terminator. The resulting sequence
535 was ordered as a dsDNA fragment from Twist Biosciences and cloned into a custom backbone.
536 This modular amilCP construct is used as a positive control for makeTCR assemblies; full
537 construct sequence details are available from Addgene (plasmid #233942). The amilCP
538 modular control vector was prepared as miniprepped plasmid, and this was further amplified
539 by RCA and assembled into the makeTCR third generation lentiviral backbone in a BsmBI
540 mediated Golden Gate reaction according to the manufacture's guidelines (plasmid
541 #233943). Assemblies were transformed into NEB stable bacteria, plated on agar and grown
542 overnight at either 30°C or 37°C before allowing the chromoprotein to mature at room
543 temperature (n=4 independent assemblies per condition, 3 technical replicates per
544 assembly).

545 **Manufacture of BsmBI site flanked germline V gene modules**

546 Germline TR*V sequences were codon optimised using human codon utilisation frequencies
547 to remove binding sites for the IIs restriction enzyme BsmBI (CGTCTC) required for TCR
548 assembly using custom R scripts. To ensure maximal downstream compatibility we also
549 depleted an additional IIs enzyme BsaI (GGTCTC), the nickase Nt.BbvCI sequence (CCTCAGC,
550 required for the isothermal DNA reading method of DNA amplification), and the rare cutter
551 SmiI/SwaI (ATTTAAAT) to allow for post Golden Gate assembly linearisation of unassembled
552 input material. Sequences were ordered as dsDNA fragments from either Twist Biosciences
553 or Integrated DNA Technologies (IDT) and assembled into the 'pMC' custom backbone vector
554 by BsaI mediated Golden Gate assembly. Full vector sequences are available in
555 Supplementary Data Table 1, as well as from Addgene and the European Plasmid Repository
556 (submitted).

557 **RCA mediated amplification of V gene modules**

558 1 ng of each germline V gene plasmid was amplified according to the manufacturer's
559 instructions by randomly primed RCA using New England Biolab's phi29-XT RCA kit in a total
560 volume of 20 µl. Prior to bead purification reactions were diluted 1:5 with nuclease free water
561 to avoid clumping of high molecular weight DNA in the subsequent magnetic bead cleanup
562 (AMPureXP Beckman Coulter). Beads were added to the reaction (0.6X bead to reaction
563 volume) and purification was completed according to the manufacturer's instructions.

564 **Rapid TCR cloning using annealed oligos**

565 Oligos encoding the CDR3-TR*J region were synthesised with a 5' phosphate moiety using a
566 SYNTAX device (DNA Script SAS). Forward and reverse oligos encoding a CDR3-TR*J fragment
567 were annealed in nuclease-free Duplex Buffer (30 mM HEPES, pH 7.5; 100 mM potassium
568 acetate, IDT) in a thermocycler (95°C for 2 min then cooled to 25°C over 25 mins) to generate
569 2 µM annealed dsDNA with cohesive ends compatible with the respective 4 nt makeTCR
570 TRAV/TRAC or TRBV/TRBC assembly sites. Annealed oligos were diluted to 0.2 µM in nuclease-
571 free water and then used in Golden Gate assembly reactions at twice the molar ratio of other
572 components (0.1 pmol of each annealed oligo pair, 0.05 pmol TR*V and TR*C, 0.034 pmol
573 precut vector backbone). Due to the risk of melting annealed oligos, the Golden Gate
574 assembly protocol was modified to include an initial low temperate step (25°C for 20 min),
575 followed by 30 cycles of 42°C/16°C for 1 min each, then an additional 15 min at 42°C, and a
576 final heat inactivation step at 60°C for 5 min.

577 **Generation in vitro-transcribed TCR mRNA constructs**

578 For in vitro transcription, TCRs were assembled into the makeTCR lentiviral backbone which
579 includes an optimised T7 promoter downstream of the elongation factor one alpha (EF1α)
580 promoter used to drive expression in transduced T cells [38]. A linear template for IVT reactions
581 was generated by PCR utilising 0.2 µl of the Golden Gate TCR assembly reaction in a 20 µl
582 reaction using SuperfiII polymerase (Thermo Scientific). 20 cycles of PCR were performed
583 using a Tm of 66°C using the forward primer CAGGTGTCGTGACGTTTAGTG and the reverse
584 primer GGCTGGCACGAAATTGTTG. The resulting PCR product was cleaned using AmpureXP
585 beads (0.6X ratio) and used as a template for the T7 mScript Standard mRNA Production
586 System (CELLSCRIPT C-MSC11610). mRNA was m7G capped and enzymatically polyadenylated
587 following the manufacturer's instructions.

588 **Quality control of TCRs generated from annealed oligos**

589 IVT templates for individually assembled TCRs were prepared as barcoded libraries
590 compatible with Nanopore sequencing using the Native Barcoding kit (SQK-NBD114.24,
591 Oxford Nanopore Technologies). Libraries were sequenced on Flongle flow cell (R10.4.1) on a
592 MinION Mk1D (Oxford Nanopore Technologies) for 24 h. Reads were demultiplexed and
593 basecalled using the Dorado basecaller implemented within MinKNOW, and then aligned to

594 the appropriate TCR reference sequencing using the Clara Parabricks (v4.3.2-1)
595 implementation of Minimap2 (v2.26) [39] . The Dorado basecaller assigns a quality (q-score) to
596 each read; if a read aligned to the reference sequence with fewer mismatches than would be
597 expected from the q-score then that read was called to be error-free.

598 **Isolation and expansion of REP T cells from healthy donor PBMCs**

599 PBMCs from healthy donors were isolated from heparinized blood. 15.5 ml of Ficoll Paque
600 Plus Media (Cytiva) was loaded per Leucosep tube (Greiner Bio-One). After adding 3 ml of PBS
601 (Sigma), up to 25 ml of blood was loaded on top and a density-gradient centrifugation was
602 performed at 800 g. After collection of the interphase, PBMCs were washed twice with PBS
603 and frozen in a controlled rate freezing device at −80 °C in 50 % freezing medium A (60 % X-
604 Vivo 20 and 40 % fetal calf serum) and 50 % medium B (80 % fetal calf serum and 20 %
605 dimethylsulfoxide). Cells were stored in liquid nitrogen at −140 °C until further analysis.

606 The rapid expansion protocol was used to expand T cells. PBMCs from three independent
607 donors were irradiated at 40 Gy using a Gammacell 1000 (AECL) radiation device to serve as
608 feeder cells. Then, 1×10^7 cells from each donor were pooled together, cells were spun down
609 (400 g, 10 min, room temperature) and resuspended in rapid expansion media (X-Vivo15
610 (Lonza, BE02-060Q), 2% human AB serum (H4522-100ML, Sigma-Aldrich), 2.5 µg/ml
611 Fungizone (15290-018, Gibco), 20 µg/ml gentamicin (2475.1, Roth), 100 IU/ml penicillin and
612 100 µg/ml streptomycin (15140122, Life Technologies)). Next, 150,000 PBMCs were plated
613 into a standing T25 flask and 666 ng of OKT-3 antibody (Life Technologies, 16-0037-85) was
614 added to the culture and the flask was topped up to a total volume of 20 ml. The next day,
615 5 ml of X-Vivo15 supplemented with 2 % AB serum containing 7,500 IU interleukin-2 (IL-2) was
616 added to the culture. Three days later, 12.5 ml of medium was removed and replaced with
617 12.5 ml of X-Vivo15 supplemented with 2% AB serum containing 600 IU ml−1 IL-2. We
618 estimated the REP cultures to contain between 40 and 50 % CD8+ T cells using flow cytometry.

619 **TCR reactivity screening via flow cytometry**

620 TCR-encoding RNA was electroporated into expanded healthy donor PBMCs using the Lonza
621 4D-Nucleofector (program EO-115, solution P3 supplemented according to the
622 manufacturer's recommendations). Transfected cells were plated in 48-well plates containing
623 TexMACS media (130-097-196, Miltenyi) supplemented with 2% human AB serum. At 18–24 h
624 after electroporation, cells were collected and 50 IU ml^{-1} benzonase (YCP1200-50KU, Speed
625 BioSystems) was added to avoid cell clumping. TCR expression levels were measured via flow
626 cytometry with markers including fixable viability dye (eFluor 450, eBioscience), CD3 (clone
627 HIT3A, BUV510, BD), and mTCRb (clone H57-597, PE, Biolegend).

628 To assess TCR reactivity, a total of 150,000 T cells and 75,000 cells of the patient-autologous
629 tumor cell line were cocultured in U-bottom 96-well plates in a total volume of 200 µ for 4
630 hours. Wells with only T cells, or T cells and TransAct beads (130-111-160, Miltenyi) were used
631 as negative and positive controls, respectively. Markers included fixable viability dye (eFluor

632 450, 1:1,000 dilution, eBioscience), CD3 (clone UCHT-1, BUV395, 1:100 dilution, BD), CD69
633 (Clone FN50, PE-Cy7, 1:200, Biolegend) and mTCRb (clone H57-597, 1:50 dilution, PE,
634 Biolegend). Samples were acquired on a Biorad ZE5 and flow cytometry data were analyzed
635 using FlowJo software, v10.6.2 (FlowJo LLC).

636 TCRs were classified as reactive or nonreactive based on flow cytometry data acquired after
637 coculture. The percentage of CD69 (%CD69) was quantified by gating on viable $CD3^+$ singlets.
638 TCRs were included in the analysis if the mTCRβ expression was >10%. The CD69 signal per
639 TCR after coculture with the cell line ('TCR versus cell line') or after running the coculture
640 assay without stimulation ('TCR, unstimulated') was corrected for background by calculating

641 (%CD69 TCR vs cellline − %CD69 TCR , unstimulated) − (%CD69 Mock vs cellline − %CD69 Mock,
642 unstimulated)

643 where mock refers to expanded T cells electroporated without TCR-encoding RNA. TCRs were
644 classified as reactive if the background corrected %CD69 signal per TCR was larger than 2×
645 the standard deviation of the %CD69 signal measured in all samples without stimulation.
646 Where a TCR clonotype expressed two α chains, data are presented for the α chain resulting
647 in the higher %CD69 expression (i.e. the functional pair).

648 **ssDNA oligo pool design**

649 Sequences encoding the CDR3a-TRAJ and CDR3b-TRBJ regions for each TCR were modified by
650 silent mutagenesis to remove BsmBI, PaqCI and SwaI restriction enzyme sites. In cases were
651 TCR sequences were to be analysed by nanopore long read sequencing data, homopolymer
652 runs of 6 nucleotides or more were removed by further silent mutagenesis to prevent
653 sequencing artifacts around these regions. BsmBI sites were then appended to the end of
654 each CDR3-TR*J sequence, and filler DNA added to pad all sequences to 210 nucleotides using
655 custom R code to add GC balanced random bases without introducing additional restriction
656 sites, homopolymers, or primer binding sites. Unique pairs of 20nt long primers from
657 Subramanian et al [31] were then added to the ends of the design to make a total of 250
658 nucleotides. An example sequence is shown in Extended Data Fig. 6; this strategy allowed for
659 cloning up to a combined total of 61 amino acids for CDR3a-TRAJ and CDR3b-TRBJ.

660 **Library demultiplexing PCR setup**

661 Library demultiplexing was performed in 15 µL reactions using KAPA HiFi HotStart ReadyMix
662 (Roche) with 0.05 ng of single-stranded DNA (ssDNA) oligo pool per well in a 384-well plate
663 format. The demultiplexing PCR mastermix was dispensed into 384-well plates using a
664 microfluidics based non-contact dispenser (Formulatrix Mantis). Two orthogonal primers
665 were dispensed into each well at a final concentration of 0.2 µM, directly from 100 µM 96-
666 well stock plates, using a 96-well plate based non-contact liquid handler (Dispendix I.DOT).
667 Following reaction setup, plates were centrifuged at 1,000 rcf for 1 min and subjected to
668 orbital shaking on a Bioshake iQ at 3,000 rpm for 3 min. Plates were centrifuged again prior

669 to PCR amplification in an Eppendorf x50t under the following modified conditions: an initial
670 three-step touchdown protocol starting at 65°C was implemented to enhance amplification
671 specificity, followed by 33 cycles of PCR with an annealing temperature of 62°C and an
672 extended annealing time of 40 sec to promote specific priming and efficient on-target
673 amplification despite elevated annealing temperature.

674 Post-PCR cleanup was performed using AMPure XP beads, dispensed at a 1:1 bead-to-reaction
675 volume ratio using the Formulatrix Mantis. Plates were then transferred to an Agilent Bravo
676 liquid handling system to perform a magnetic bead-based DNA purification in 384-well
677 format. PCR products were eluted in Greiner UV Star plates and post-cleanup DNA
678 concentrations were measured via absorbance (Varioska LUX Multimode Microplate Reader);
679 custom scripts were then used to normalise all wells to a uniform concentration of 1 ng/µL in
680 deep-well plates.

681 **Golden Gate mediated arrayed assembly of thousands of TCRs**

682 Golden Gate assembly of T cell receptors (TCRs) was performed using the NEBridge® Golden
683 Gate Assembly Kit (BsmBI-v2) following the manufacturer's recommendations, scaled down
684 to a reaction volume of 2 µL. Assembly reactions were prepared in 384-well plates using a
685 Dispendix I.DOT non-contact dispenser to give a ratio of 1 CDR3 oligo : 0.91 TR*V : 0.9 TR*C :
686 0.67 Vector. Corresponding αβ V gene segments, preset constant region modules, and the
687 respective vector of choice were automatically dispensed onto 1 ng of purified oligo DNA per
688 well. Following reagent dispensing, plates were mixed on a Bioshake iQ at 3,000 rpm for 3
689 min and centrifuged at 1,000 rcf for 1 min to collect the reaction. Assembly was performed in
690 an Eppendorf X50t thermal cycler using a custom temperature profile: reactions were
691 incubated at 42°C for 30 min, followed by 30 cycles of 42°C/16°C for 1 min each, then an
692 additional 30 min at 42°C, and a final heat inactivation step at 60°C for 5 min.

693 **TCR library preparation**

694 To generate the pooled plasmid library, 2 µl of each assembled TCR was combined into a
695 single well using an automated liquid handling system (Bravo, Agilent Technologies). Prior to
696 bacterial transformation, the pooled assemblies were purified using AMPure XP beads
697 (Beckman Coulter) at a bead-to-sample ratio of 0.8X to enhance electroporation efficiency.
698 Assembled plasmids were eluted in 60 µl of nuclease-free water and subsequently
699 transformed into electrocompetent *E. coli* (NEB 10-beta, New England Biolabs) following the
700 manufacturer's protocol. To minimize recombination within lentiviral long terminal repeats,
701 bacterial outgrowth was performed at 30 °C for 1 h in NEB's proprietary recovery medium.
702 Cultures were then transferred directly into selective LB medium supplemented with
703 100 µg/mL carbenicillin. To assess transformation efficiency and estimate library coverage,
704 10 µL of the outgrowth was plated on 10 cm LB-agar plates containing the same antibiotic.
705 For all transformations, a minimum of 500X library coverage was maintained. Cultures were

706 expanded at 30 °C for 16–24 h prior to plasmid extraction using a ZymoPURE II Plasmid
707 Maxiprep Kit (Zymo Research).

708 **Nanopore sequencing of large TCR libraries**

709 0.01 ng of generated plasmid libraries were used as input for amplicon generation to add UMI
710 adapters to the end of constructs as described by Amstler et al., 2024. UMIs were
711 incorporated by two cyles of PCR (2 min extension at 72°C, 30 s annealing at 60°C) with
712 Platinum SuperFi II PCR Master Mix (Invitrogen) using 0.01 ng of the prepared TCR library and
713 0.5 nM of primers
714 GTCTCTGCTCGACTAACCACTTTVVVVVTVTTVVVVTTVVVTTGTGTGGCTGGCACGAAATTG and
715 GCTCTCATACGAACTCGTCCTTTVVVVVTTVVVTTVVVVTTVVVVTTTAAGTGCAGTAGTCGCCGTG
716 (IDT, machine mixed random bases incl. PAGE-purification. This amplicon was then purified
717 with magnetic beads (Ampure-XP Beckman Coulter, 0.8x ratio). Subsequently, the UMI-
718 tagged product was subjected to a second PCR using Platinum SuperfiII polymerase
719 (Invitrogen) with universal primers binding the last 20 bases of both 5' adaptors of the UMI
720 primers. 0.5 nM of either primer (GCTCTCATACGAACTCGTCC, GTCTCTGCTCGACTAACCAC)
721 was used to amplify the product derived from PCR1 for 25 cycles (annealing 60 °C, 10 s,
722 extension 72 °C 60 s). Nanopore compatible libraries were then generated using either the
723 Ligation sequencing kit (SQK-LSK114) or the Native Barcoding kit (SQK-NBD114.24, Oxford
724 Nanopore Technologies) and sequenced on a PromethION 2 Solo device for three days using
725 a PromethION Flow Cell R10.4.1 or a flongle (R10.4.1) on a Mk1D for 24 h. To reduce compute
726 time we implemented Clara Parabricks (v4.3.2-1) to run Minimap alignments on CUDA
727 GPUs[39]. Secondary and supplementary alignments were subsequently filtered from the
728 generated bam file using samtools [41].

729 **Calculation of correct assembly rate**

730 The assembly rate was calculated as follows: when sequencing pooled, high-throughput
731 manufactured TCRs amplicon reads were first anchored to a TCR reference by filtering for
732 reads containing a perfect alignment to the first and last ten nucleotides of a TCR (thereby
733 depleting reads mapping to residual empty vector that could not be assigned to any one TCR
734 assembly). When sequencing barcoded TCRs generated by rapid TCR assembly this filtering
735 was not required as reads could be mapped to the correct reference TCR by the barcode
736 (derived from the SQK-NBD114.24 kit). Phred scores of the aligned fraction of reads were
737 converted to error probabilities (10^(-Q_score/10); as described by Edgar and Flyvbjerg [42] the
738 expected error rate for each read was characterized by the sum of error probabilities of the
739 alignment region to the reference rounded to the nearest lower integer. The expected error
740 rate was compared to the NM tag of the alignment allowing an estimation of the edit distance
741 between a respective read and its cognate reference (observed errors within the read). Reads
742 with fewer observed errors than expected on the basis of read quality were classified as a
743 perfect assembly; the ratio of perfect assemblies to the number of reads aligning to a
744 particular reference represents the assembly rate.

745 **Assessment of cloning fidelity**

746 When sequencing pooled, high-throughput manufactured TCRs amplicon reads were first
747 aligned against all full-length TCR reference sequences to establish the ground truth TCR for
748 each read. When sequencing barcoded TCRs generated by rapid TCR assembly this filtering
749 was not required as reads could be mapped to the correct reference TCR by the barcode
750 (derived from the SQK-NBD114.24 kit). In both cases reads were then aligned to individual
751 TCR sub-sequences (TRAV, TRBV, CDR3a, CDR3b, TRAC, and TRBC-T2A). Read IDs and their
752 respective reference assignments were extracted from the BAM file, merged, and then
753 compared to evaluate cloning fidelity for each reference. For each individual segment, the
754 percentage of on-target reads aligning to the correct reference was determined (i.e. if a TCR
755 utilised TRBV10-1, what % of reads for this TCR mapped to TRBV10-1).

756 **Quality controlling CDR3-J oligos post PCR demultiplexing**

757 To identify primer off-target binding resulting in incorrect TCR assembly we performed
758 Nanopore sequencing, preparing 100-200 fmol of purified demultiplexed PCR amplicons for
759 sequencing using Oxford Nanopore Technologie's native barcoding kit (SQK-NBD114.24).
760 Barcoded samples were loaded on a flongle flowcell (R10.4.1) and sequenced for 24 h.
761 Alignment against a reference of all oligos within a given library was performed using Clara
762 Parabricks v4.3.2-1 (Minimap2 v2.26) [39], and primer sequences were detected in reads using
763 flexiplex [43]. Off-target primer binding was examined using Tablet[44] and Snapgene software.

764 **References**

765 1. D'Angelo, S. P. *et al.* Afamitresgene autoleucel for advanced synovial sarcoma and
766 myxoid round cell liposarcoma (SPEARHEAD-1): an international, open-label, phase 2
767 trial. *The Lancet* **403**, 1460–1471 (2024).

768 2. Wermke, M. *et al.* Autologous T cell therapy for PRAME+ advanced solid tumors in HLA-
769 A*02+ patients: a phase 1 trial. *Nat Med* (2025) doi:10.1038/s41591-025-03650-6.

770 3. Zacharakis, N. *et al.* Immune recognition of somatic mutations leading to complete
771 durable regression in metastatic breast cancer. *Nat Med* **24**, 724–730 (2018).

772 4. Foy, S. P. *et al.* Non-viral precision T cell receptor replacement for personalized cell
773 therapy. *Nature* **615**, 687–696 (2023).

774 5. Pogorelyy, M. V *et al.* TIRTL-seq: Deep, quantitative, and affordable paired TCR
775 repertoire sequencing. doi:10.1101/2024.09.16.613345.

776 6. Pogorelyy, M. V. *et al.* Detecting T cell receptors involved in immune responses from
777 single repertoire snapshots. *PLoS Biol* **17**, 1–13 (2019).

778 7. Lowery, F. J. *et al.* Molecular signatures of antitumor neoantigen-reactive T cells from
779 metastatic human cancers. *Science (1979)* **375**, 877–884 (2022).

780 8. Caushi, J. X. *et al. Transcriptional Programs of Neoantigen-Specific TIL in Anti-PD-1-*
781 *Treated Lung Cancers*. *Nature* vol. 596 (Springer US, 2021).

782 9. Zheng, C. *et al.* Transcriptomic profiles of neoantigen-reactive T cells in human
783 gastrointestinal cancers. *Cancer Cell* **40**, 410-423.e7 (2022).

784 10. Meng, Z. *et al.* Transcriptome-based identification of tumor-reactive and bystander
785 CD8 + T cell receptor clonotypes in human pancreatic cancer . *Sci Transl Med* **15**, 1–19
786 (2023).

787 11. Zeng, Z. *et al.* A minimal gene set characterizes TIL specific for diverse tumor antigens
788 across different cancer types. *Nat Commun* **16**, 1070 (2025).

789 12. Tan, C. L. *et al.* Prediction of tumor-reactive T cell receptors from scRNA-seq data for
790 personalized T cell therapy. *Nat Biotechnol* (2024) doi:10.1038/s41587-024-02161-y.

791 13. Pétremand, R. *et al.* Identification of clinically relevant T cell receptors for personalized
792 T cell therapy using combinatorial algorithms. *Nat Biotechnol* (2024)
793 doi:10.1038/s41587-024-02232-0.

794 14. Fast, E., Dhar, M. & Chen, B. TAPIR: a T-cell receptor language model for predicting rare
795 and novel targets. *bioRxiv* 2023.09.12.557285 (2023) doi:10.1101/2023.09.12.557285.

796 15. Drost, F. *et al.* Predicting T cell receptor functionality against mutant epitopes. *Cell*
797 *Genomics* (2024) doi:10.1016/j.xgen.2024.100634.

798 16. Dolton, G. *et al.* Targeting of multiple tumor-associated antigens by individual T cell
799 receptors during successful cancer immunotherapy. *Cell* 1–17 (2023)
800 doi:10.1016/j.cell.2023.06.020.

801 17. Boschert, T. *et al.* H3K27M neoepitope vaccination in diffuse midline glioma induces B
802 and T cell responses across diverse HLA loci of a recovered patient. *Sci Adv* **10**, 9091
803 (2024).

804 18. Guo, X. zhi J. *et al.* Rapid cloning, expression, and functional characterization of paired
805 αβ and γδ T-cell receptor chains from single-cell analysis. *Mol Ther Methods Clin Dev* **3**,
806 15054 (2016).

807 19. Moravec, Z. *et al.* Discovery of tumor-reactive T cell receptors by massively parallel
808 library synthesis and screening. *Nat Biotechnol* (2024) doi:10.1038/s41587-024-02210-
809 6.

810 20. Hu, Z. *et al.* A cloning and expression system to probe T cell receptor specificity and
811 assess functional avidity to neoantigens. *Blood* **132**, blood-2018-04-843763 (2018).

812 21. Zong, S. *et al.* Very rapid cloning, expression and identifying specificity of T-cell
813 receptors for T-cell engineering. *PLoS One* **15**, (2020).

814 22. Pryor, J. M. *et al.* Enabling one-pot Golden Gate assemblies of unprecedented
815 complexity using data-optimized assembly design. *PLoS One* **15**, 1–19 (2020).

816 23. Liljeruhm, J. *et al.* Engineering a palette of eukaryotic chromoproteins for bacterial
817 synthetic biology. *J Biol Eng* **12**, 1–10 (2018).

818 24. Cohen, C. J. *et al.* Enhanced antitumor activity of T cells engineered to express T-cell
819 receptors with a second disulfide bond. *Cancer Res* **67**, 3898–3903 (2007).

820 25. Bethune, M. T. *et al.* Domain-swapped t cell receptors improve the safety of TCR gene
821 therapy. *Elife* **5**, 1–24 (2016).

822 26. Degirmencay, A. *et al.* Exploitation of CD3ζ to enhance TCR expression levels and
823 antigen-specific T cell function. *Front Immunol* **15**, (2024).

824 27. Bolotin, D. A. *et al.* MiXCR: software for comprehensive adaptive immunity profiling.
825 *Nat Methods* **12**, 380–381 (2015).

826 28. Marano, J. M., Chuong, C. & Weger-Lucarelli, J. Rolling circle amplification: A high
827 fidelity and efficient alternative to plasmid preparation for the rescue of infectious
828 clones. *Virology* **551**, 58–63 (2020).

829 29. Hejazi, S., Ahsan, A., Kashani, S. M., Tameiv, D. & Reuel, N. F. Amplified DNA
830 heterogeneity assessment with Oxford Nanopore sequencing applied to cell free
831 expression templates. *PLoS One* **19**, (2024).

832 30. Cetin, M. *et al.* T-FINDER: A highly sensitive, pan-HLA platform for functional T cell
833 receptor and ligand discovery. *Sci Adv* **10**, 1–12 (2024).

834 31. Subramanian, S. K., Russ, W. P. & Ranganathan, R. A set of experimentally validated,
835 mutually orthogonal primers for combinatorially specifying genetic components. *Synth*
836 *Biol* **3**, 1–5 (2018).

837 32. Gotti, E. *et al.* Optimization of therapeutic T cell expansion in G-Rex device and
838 applicability to large-scale production for clinical use: GMP-compliant polyclonal T cell
839 expansion in G-Rex. *Cytotherapy* **24**, 334–343 (2022).

840 33. Sahillioglu, A. C. & Schumacher, T. N. Safety switches for adoptive cell therapy. *Current*
841 *Opinion in Immunology* vol. 74 190–198 Preprint at
842 https://doi.org/10.1016/j.coi.2021.07.002 (2022).

843 34. Afeyan, A. B., Wu, C. J. & Oliveira, G. Rapid parallel reconstruction and specificity
844 screening of hundreds of T cell receptors. *Nat Protoc* (2024) doi:10.1038/s41596-024-
845 01061-4.

846 35. Barreira, M. *et al.* Enzymatically amplified linear dbDNATM as a rapid and scalable
847 solution to industrial lentiviral vector manufacturing. *Gene Ther* **30**, 122–131 (2023).

848 36. Meysman, P. *et al.* Benchmarking solutions to the T-cell receptor epitope prediction
849 problem: IMMREP22 workshop report. *ImmunoInformatics* **9**, 100024 (2023).

850 37. Xia, Q. H. H. D. M. M. A High-Throughput Strategy for T-Cell Receptor Cloning and
851 Expression. in *Methods in Molecular Biology - T-Cell Repertoire Characterization* vol.
852 2574 251–264 (2022).

853 38. Conrad, T., Plumbom, I., Alcobendas, M., Vidal, R. & Sauer, S. Maximizing transcription
854 of nucleic acids with efficient T7 promoters. *Commun Biol* **3**, 1–8 (2020).

855 39. NVIDIA. Clara Parabricks . Preprint at (2019).

856 40. Amstler, S. *et al.* Nanopore sequencing with unique molecular identifiers enables
857 accurate mutation analysis and haplotyping in the complex lipoprotein(a) KIV-2 VNTR.
858 *Genome Med* **16**, 117 (2024).

859 41. Danecek, P. *et al.* Twelve years of SAMtools and BCFtools. *Gigascience* **10**, (2021).

860 42. Edgar, R. C. & Flyvbjerg, H. Error filtering, pair assembly and error correction for next-
861 generation sequencing reads. *Bioinformatics* **31**, 3476–3482 (2015).

862 43. Cheng, O. *et al.* Flexiplex: a versatile demultiplexer and search tool for omics data.
863 *Bioinformatics* **40**, (2024).

864 44. Milne, I. *et al.* Using tablet for visual exploration of second-generation sequencing data.
865 *Brief Bioinform* **14**, 193–202 (2013).

866